NASA Technical Memorandum 4181

Water-Tunnel Investigation of Concepts for Alleviation of Adverse Inlet Spillage Interactions With External Stores

Dan H. Neuhart
Lockheed Engineering & Sciences Company
Hampton, Virginia

Matthew N. Rhode
Langley Research Center
Hampton, Virginia

National Aeronautics and
Space Administration
Office of Management
Scientific and Technical
Information Division

1990

Summary

A test was conducted in the NASA Langley 16- by 24-Inch Water Tunnel to study alleviation of the adverse interactions of inlet spillage flow with the external stores of a fighter aircraft. A 1/48-scale model of a fighter aircraft was used to simulate the flow environment around the aircraft inlets and on the downstream underside of the fuselage. A controlled inlet mass flow was simulated by drawing water into the inlets. Various flow control devices were used on the underside of the aircraft model to manipulate the vortical inlet spillage flow.

Introduction

This test was initiated to investigate the vortical inlet spillage flow created when the inlet mass flow ratio on a fighter aircraft is reduced below a value of 1.0. Under these conditions, the cross-sectional area of the inlet stream tube is less than the projected area of the inlet. The inlet mass flow ratio is the ratio of the mass flow in the inlet stream tube to the theoretical mass flow in a stream tube with a cross-sectional area equal to the projected area of the inlet. In the present study, the inlet mass flow ratio was maintained at 0.25, simulating a condition where the thrust is substantially reduced from cruise (a "throttle chop" to idle, for example). As the flow approaches the inlet, the streamlines diverge and some of the flow "spills" around the inlet, resulting in unsteady, vortical flow that moves downstream underneath the aircraft surface. This vortical flow can interact with control surfaces, stores, pods, fuel tanks, and any external surface, as illustrated in figure 1. This interaction is generally adverse, both in terms of potential structural damage and creation of undesirable aerodynamic flow field interactions. Therefore, some method of alleviation is desired to neutralize or at least minimize the adverse interactions of the vortical flow produced by inlet spillage.

Vortex flow alleviation was approached in two ways: deflection of the flow by physical barriers or by the creation of auxiliary vortex flows to interact with local flows. The purpose of the first approach was to use ventral fins to deflect or confine the vortical inlet spillage flow from the outboard missile carriage locations, as shown in figure 2. The purpose of the second approach was to generate vortex flows to neutralize ("unwind"), induce a favorable displacement of, or deform and deflect the vortical spillage flows. No attempt was made to address the effects of these alleviation methods on aircraft stability and control or aircraft drag.

Vortex flows in general are characterized by a tangential (rotational) velocity profile, as shown in figure 3. The vortex core region exhibits a linear growth in velocity with increasing distance from the center. Outside the core region, the velocity is inversely proportional to the distance from the vortex center. Therefore, in this "potential vortex" region, the tangential velocity influence diminishes rapidly. In real viscous flow, the velocity "peak" is more rounded than shown in this schematic drawing and the boundary of the core region is less distinct.

One way to neutralize or "unwind" a vortex flow is to introduce a vortex flow of opposite rotation and equal magnitude. Figure 4 shows an example of an idealized flow where positive and negative velocities cancel each other, and the net tangential velocity is zero. In a real situation, if one of the vortex flows had higher velocities, then some residual circulation, greatly reduced from the original flow, would remain. McGinley and Beeler (ref. 1) examined vortex unwinding on a flat plate in a wind tunnel. Their results indicate that vortices can be countered and, in fact, were slightly overcompensated by their unwinders.

Another method of vortex control is by mutual induction. Two vortices of opposite rotation, when adjacent to each other, induce velocities on each other that cause them to advance in the manner shown in figure 5. When the two vortices are of equal strength, they translate along a straight path perpendicular to the line between their centers, as depicted in figure 5(a). The schematic shown in figure 5(b) indicates that when one vortex is stronger the path is curved toward the stronger vortex. These two examples of induction illustrate a method for moving an adverse vortex flow away from a critical area on the aircraft surface.

Deformation and displacement of a vortex flow can be accomplished by generating a second vortex with the same direction of rotation. As shown in figure 6(a), the two vortices, by their mutual influence on each other, rotate around each other and begin to deform as a preliminary stage of vortex merging. This deformation makes the vortex more diffuse. If the generated vortex is of greater strength than the original vortex, it will tend to cause the original vortex to rotate around it and greatly deform (fig. 6(b)). Vortex merging has been studied by many researchers, especially in relation to aircraft wake vortex alleviation. Two examples are the studies by Bilanin et al., reference 2, and Brandt and Iversen, reference 3.

Symbols

A_I	inlet stream tube area, ft^2
A_{proj}	projected inlet area, ft^2
$\dot{m}_I$	inlet mass flow rate, $\rho A_I V_I$, slugs/sec

$\dot{m}_\infty$	free-stream mass flow rate, $\rho A_{\text{proj}} V_\infty$, slugs/sec
V_I	velocity in the inlet stream tube, ft/sec
V_∞	free-stream velocity, ft/sec
α	angle of attack, deg
β	angle of sideslip, deg
ρ	fluid density, slugs/ft^3

Test Setup and Method

Test Facility

The NASA Langley 16- by 24-Inch Water Tunnel is shown in figure 7. The tunnel has a vertical test section with an effective working length of about 4.5 ft. The velocity in the test section can be varied from 0 to 0.75 ft/sec, resulting in unit Reynolds numbers from 0 to 7.73×10^4 ft^{-1} based on a water temperature of 78°F. The normal test velocity yielding smooth flow is 0.25 ft/sec, resulting in unit Reynolds numbers of 2.58×10^4 ft^{-1} at 78°F and 2.29×10^4 ft^{-1} at 68°F.

The model support system has deflection ranges of ±33° and ±15° in two planes of rotation. Rotation is accomplished by electronic remote control, and visual indicators allow the user to set angles within about ±0.25°.

The flow visualization method for this investigation used colored dye injected into the flow field from orifices in the model.

Model

The model used was a 1/48-scale model of a twin-engine fighter aircraft, shown in figure 8. A line drawing giving the basic dimensions of the model is shown in figure 9. The external geometry of the model was generally representative of a full-scale aircraft, excepting the nozzles, which had extensions to allow connection of tubing for drawing water through the inlets. The model had a centerline fuel tank and four missile-type stores mounted on the lower outside corner of the body under the wing. These stores were mounted two to a side in series, with the nose of the forward store located just aft of the inlet lower lip. The flow control devices are shown in figure 10. These devices were all made of brass plate 0.020 in. thick. Dye for flow visualization was introduced into the flow from internal dye ports in the model and from dye tubes attached externally to the model underside between the inner inlet sides and the fuselage.

Test Method

The tests were run at a free-stream velocity V_∞ of 0.25 ft/sec. For most of the tests, the water temperature stabilized at 68°F, giving a unit Reynolds number of 2.29×10^4 ft^{-1}. Based on the wing mean geometric chord, the test Reynolds number was 8.4×10^3. When the test section flow was stabilized at the test velocity, the model was set to $\alpha = 0°$ and $\beta = 0°$. The inlet mass flow rate was set with a needle valve while monitoring the flowmeter frequency on a digital counter. The desired inlet mass flow ratio of 0.25 was set by first calculating the mass flow required at an inlet mass flow ratio of 1.0. Given the projected inlet area and the free-stream velocity and density, the required mass flow rate can be calculated from the following equation:

$$\dot{m}_I = 0.25\dot{m}_\infty = 0.25\rho A_{\text{proj}} V_\infty$$

Flow visualization data were recorded using still color photography and color video. Still photographs were taken on 70-mm color negative film and printed in an 8- by 10-in. format. Generally, all attitudes were recorded from one viewpoint with one camera. The camera was then moved to a new viewpoint, and the model was returned to its original position to avoid any effects of hysteresis that might result from changing the model attitude in reverse direction. In addition, after the attitude was changed, a pause of several seconds was necessary to allow effects of the dynamic response of the flow field to the change to dissipate.

When all the desired visual data were recorded, any areas of specific interest were reexamined to check for repeatability and to analyze any phenomena that may have been difficult to interpret or resolve using the recording media. This was of particular interest for regions of the flow that were too small to accurately record and for aspects of the flow whose unsteady nature could not be conveyed appropriately on film.

Analysis and Discussion

The primary data used in the analysis of results are still photographs. Because of the qualitative nature of this study, no attempt was made to derive any quantitative information from the photographs. Observations of the rotational direction of vortical flows were made during the test, but the direction of rotation cannot be easily determined from the photographs. However, the verbal descriptions and accompanying photographs should give the reader a good understanding of the results.

Baseline Configuration

Figure 11 shows the inlet spillage flows as visualized by colored dye. The effect of angle of attack on spillage vortex trajectory was found to be small. Figure 11(a) shows the spillage vortex flowing from the inboard side of the left inlet. The dye streaks marking the two flows labeled in this figure originate from dye tubes located between the inner inlet sides and the fuselage. Figure 11(b) shows a close-up side view where the dye, injected from ports in the fuselage nose upstream of the inlet, is caught up into the vortical spillage flowing around the inlet. This vortex, flowing around the inlet face to the underside of the model, is the outboard vortex of a pair of spillage vortices discovered on this side. Figure 11(c), a right side view of the model, shows separated spillage flow on the outer vertical side of the right inlet. In addition, the inlet spillage vortex flow from the left inner inlet edge is shown underneath the model.

In figures 11(a) and (c), dye was introduced at the inboard corner of the left inlet lower lip and was immediately taken into the inner vortex flow. The direction of rotation is determined by referring to figure 1. In figure 11(a), dye was introduced on the inboard side of the right inlet in the small channel between the inlet and the forebody. As shown, this dye, which remains on the fuselage underside surface, is moved outboard relative to the dye from the left inlet which is in the vortex off the surface. This is consistent with the direction of rotation shown in figure 1 for the right side since the vortex flow would tend to sweep the surface flow outboard. Again, no effect of angle of attack was observed.

The trajectory of the vortical flow from the left inlet in figure 11(a) indicates a probable interaction with the control surfaces on the aft store. At this condition, with the model yawed to the left, the centerline fuel tank and its pylon are at an incidence and produce a wake recirculation region, dicussed later in this paper, that deflects the spillage vortex into the missile stores. In addition, the vortex flow is deflected vertically over the wake of the fuel tank and pylon and is therefore lifted away from the surface, as shown in figure 11(c).

Ventral Fins

The first device that was studied was a ventral fin deflection device. The fins were mounted perpendicular to the undersurface of the model as shown in figure 2. Fins with a height extending from the fuselage to the fuel tank centerline (one on each side) were tried initially. As shown in figure 12, with the model at $\beta = 10°$, the fin intercepts the vortex and alters its trajectory. However, at $\beta = 5°$ the fin is too far forward to appreciably affect the vortex trajectory, as shown in figure 13. (The angles of attack, although different, were not found to have an effect on the vortex trajectory in the range examined.) Next, the fin was moved aft as shown in figure 14. However, at $\beta = 5°$, there is still not enough deflection of the vortex to prevent interaction with the aft missile. Two ventral fins were tried (the forward fin having half the height of the aft fin) and appeared to offer some deflection. However, as shown in figure 15, there is still not enough modification of the trajectory to prevent serious interaction with the stores. Moreover, two ventral fins may actually make flow interactions more significant at higher sideslip angles, as shown in figure 16 (compare with fig. 12). In this case, the aft fin causes the vortex to go between the fins. One long, solid ventral fin with taper might be a better alternative to discrete fins but may also result in large performance penalties in terms of skin friction and profile drag. Therefore, a different approach (vortex unwinders) was taken that appeared to be less sensitive to model attitude.

Vortex Unwinders

As previously stated, the second approach involves creation of auxiliary flows to interact with the original vortex flows. The concept of vortex unwinders was investigated because of their potential for neutralizing these vortex flows. The generating surfaces tested in this study were placed on the inboard side of the inlets in the channel between the inlets and the forebody, as shown in figure 17. They were placed at a negative angle of attack relative to the model centerline to produce a tip vortex of opposite rotation to the spillage vortex flow. The first configuration had a rectangular planform and was placed downstream of the inlet lower lip. Figure 18(a) shows the resultant dye streak path of the spillage flow. The spillage vortex was deflected and somewhat diffused, but the unwinder was too far from the source of the spillage vortex to be properly aligned with it. The device was moved forward and, as shown in figure 18(b), the spillage flow was drawn into the device tip vortex. Although the still photograph cannot show the vortex sense of rotation, observations at the time of testing clearly showed the initial sense of rotation of the spillage vortex to be completely reversed by the unwinder. This of course means that the unwinder was oversized since the resultant vortex flow had residual opposite rotation. A smaller device, with a triangular planform forming a semidelta wing, was tested next. This vortex unwinder had the advantage of providing reduced area and therefore reduced vortex strength as well as less flow blockage in the channel where it was located. Figure 19 shows the results.

The original vortex flow was still overcompensated; however, the residual vortex flow was less energetic and more diffuse. In a detailed design, proper sizing could resolve the overcompensation by determining the spillage flow vortex strength.

Vortex Induction

The method of providing an opposite-rotation vortex to induce the spillage vortex away from the stores was tried next. The devices used were fins attached to the centerline fuel tank. As shown in figure 20, they were positioned nose-up toward the fuselage to provide a flow of opposite rotation close to the source of the spillage vortex flow. As shown in figure 21, test results with this device showed negligible, if any, effect on the spillage flow. Comparison of figure 21 with figure 11(a) shows an almost identical trajectory, although the induction fin may have caused the vortex to be more diffuse because of a weak, remote, shearing influence. A disadvantage of this device is that the fin lift vector points toward the aircraft. When jettisoning the fuel tank, the lift force on the fins could cause an impact between the fuel tank and the aircraft. The advantage, however, of this device and of the following device is that, since the presence of the centerline fuel tank appears to deflect the spillage flow into the missile stores, these devices need only be present when the fuel tank is mounted to the aircraft, since they are attached to the tank.

Vortex Deformation and Displacement

The devices for producing vortex deformation and displacement were initially similar in location and opposite in attitude compared with the previous (vortex induction) devices. To provide a rotation of the same direction as the spillage vortex, these fins were oriented with their leading edges away from the body (at a negative angle of attack) as shown in figure 22.

Figures 23(a) and (b) show two views with the fins forward on the fuel tank. These photographs can be compared to figures 11(a) and (c), respectively. In figures 23(a) and 11(a), it can be seen that the dye streak is initially spread out by the fin. The side views, figures 23(b) and 11(c), show that the spillage vortex is displaced from the model lower surface, near the center of the fuel tank, by the fin.

In an attempt to provide a stronger effect, the fins were enlarged and moved aft to interact with the vortex as it rises. Figure 24 shows the results. (Two planform shapes were tried, rectangular and triangular, and both produced similar effects.) The spillage is more strongly deflected both horizontally and vertically. In addition, although not visible in the photographs, the vortices were often quite diffuse, indicating significant deformation as they were stretched around the fin vortex.

The fin orientation would provide a fin lift vector directed away from the aircraft, possibly assisting fuel tank jettison as long as the loads do not put too much stress on the tank pylon. The size of the fins would need to be optimized to minimize drag while maintaining the desired vortex effect.

Test Limitations

Although this is a qualitative study, several points need to be considered concerning aspects of the full-scale flow that are not modeled in the water tunnel. This is important in extrapolating even qualitative results to full-scale configurations. The ratio of full-scale to water-tunnel Reynolds numbers is about 1000 to 1. The effect of the low test Reynolds number manifested itself in several areas. Figure 25(a) shows a large wake region aft of the centerline fuel tank. When the model was yawed, this region became asymmetric and produced the large recirculation region shown in figure 25(b) (the ventral fins on the model in this view did not alter the occurrence of the recirculation region). This region clearly has an effect on the spillage vortex trajectory, both horizontally and vertically. The wake will exist for the full-scale aircraft, but it will be significantly smaller and have less effect on the vortex trajectory.

Calculations of flat-plate boundary-layer thickness over the distance from the inlet lower lip to the aft missile forward fin root leading edge showed that the scaled-up laminar boundary-layer thickness is 6.2 times greater than the full-scale, flat-plate, turbulent boundary-layer thickness. This implies that the water-tunnel flow is deflected away from the fuselage surface more in a relative sense than at full scale, and that some devices may be largely or completely immersed in the water-tunnel model boundary-layer flow, depending on their location.

All attached flow in the water tunnel is laminar. The full-scale flow is probably completely turbulent, more energetic, and better able to resist separation. However, this implies that the water-tunnel flow provides a "worst case" scenario for flows that can be simulated. If a flow problem can be solved or improved upon at low Reynolds numbers, it can likely be improved at high Reynolds numbers.

Finally, no compressibility effects can be simulated in the water tunnel. Even for subsonic full-scale flight conditions, regions of local high-speed compressible flow will not be modeled.

Although the above limitations seem quite restrictive, it is important to note that the qualitative character of the flow will generally be modeled. And, as mentioned previously, if a flow problem can be simulated and solved in the water tunnel, it will probably be solvable at higher Reynolds numbers.

Conclusions

A flow visualization test was conducted to study inlet spillage flow effects on a fighter aircraft model in the Langley 16- by 24-Inch Water Tunnel. The model was tested at a Reynolds number based on mean geometric chord of 8.4×10^3. The purpose of the study was to investigate the potential for alleviation of the adverse interactions of vortical inlet spillage flows with external stores. Several devices were tested to deflect the spillage flows or create auxiliary vortex flows to interact with these flows. The objectives of the test were met, and the following conclusions may be drawn.

Device Performance

Ventral fins. The ventral fins of the current study caused some deflection of the spillage vortex, but their performance depended upon model attitude. To ensure effective vortex deflections over a range of attitudes, ventral fins would probably need to be very long. This may yield performance penalties in terms of skin friction and profile drag. They may also affect lateral and directional stability in desirable or undesirable ways. They would always be present whether needed or not.

Vortex unwinders. The vortex unwinders used in this study showed significant modification of the vortical spillage flow when properly placed. Since these are placed near the source of the spillage vortex, they can be small. Their placement also has the advantage that they are less sensitive to attitude changes since the source of the spillage vortex is fixed. With proper optimization, these devices could completely neutralize the vortex. They may cause high local velocities and/or blockage in the channel area between the inboard side of the inlet and the fuselage, which would be especially troublesome at transonic speeds. They would always be present, needed or not.

Vortex induction by fuel tank fins. The vortex induction devices of the current study were ineffective, probably because of their distance from the spillage vortex. Since the tangential vortex velocity diminishes as the inverse of the distance, the influence of the device vortex diminishes rapidly. In addition, these devices, which had positive angle of attack relative to the fuselage, would have a lift vector pointing toward the aircraft. This would be a problem when jettisoning the fuel tank.

Vortex deformation and displacement by fuel tank fins. These devices were at least as effective as the vortex unwinders. Their effect on the spillage vortex was to significantly deform it by laterally stretching it around the fin vortex. They performed their function best when in the aft position. In addition, since they are mounted on the centerline fuel tank, and the fuel tank deflects the spillage vortex into the stores, they are not needed and will not be on the aircraft when the centerline fuel tank is not mounted. This makes them more desirable than devices that are always mounted to the aircraft. Because of their nose-down orientation, their lift vector points away from the aircraft and might be helpful when jettisoning the fuel tank. This may add stress to the tank pylon at high speeds, however. The fin size would need to be optimized to reduce drag for a given vortex effect.

Qualifications

All results must be evaluated with reference to the test limitations. However, the spillage flow will qualitatively behave in flight as it did in the water tunnel since the spillage vortex will form independent of Reynolds number.

None of the devices have been optimized for size, orientation (angle), or position. Only their potential for alleviating the spillage interaction problem has been demonstrated. It is felt that optimization should be performed in an environment where the previously stated limitations do not exist or will be minimized.

NASA Langley Research Center
Hampton, VA 23665-5225
March 12, 1990

References

1. McGinley, Catherine B.; and Beeler, George B.: Vortex Unwinding in a Turbulent Boundary Layer. *J. Aircr.*, vol. 24, no. 3, Mar. 1987, pp. 221–222.
2. Bilanin, Alan J.; Teske, Milton E.; Donaldson, Coleman duP.; and Snedeker, Richard S.: Viscous Effects in Aircraft Trailing Vortices. *Wake Vortex Minimization*, NASA SP-409, 1977, pp. 61–128.
3. Brandt, Steven A.; and Iversen, James D.: Merging of Aircraft Trailing Vortices. AIAA Paper 77-8, Jan. 1977.

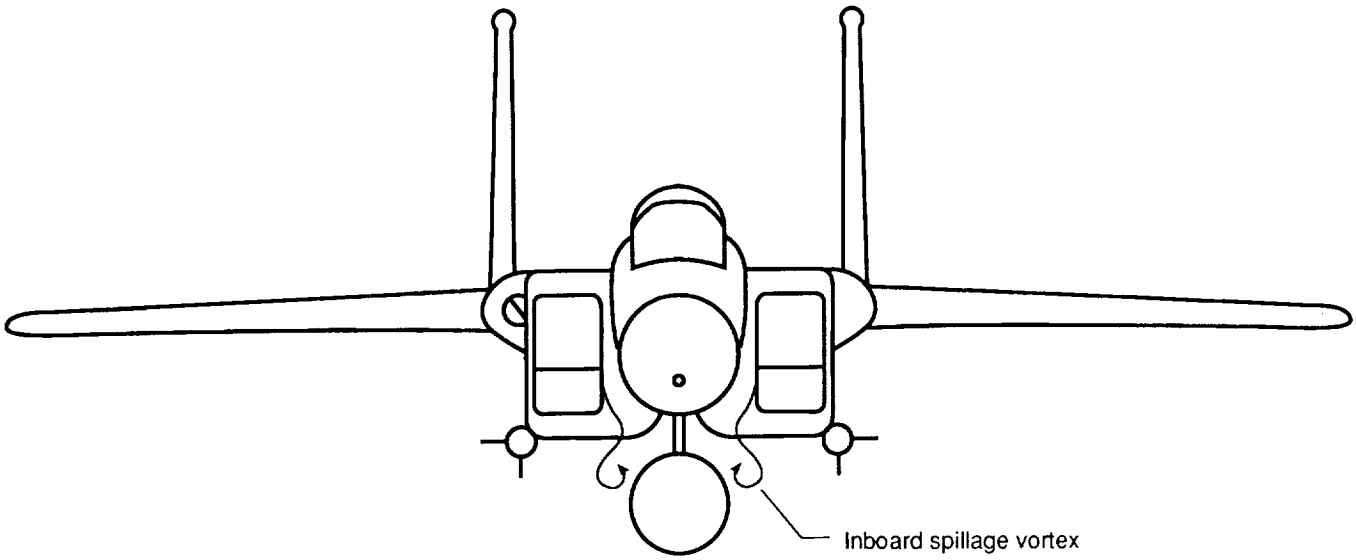

Figure 1. Inlet spillage flow.

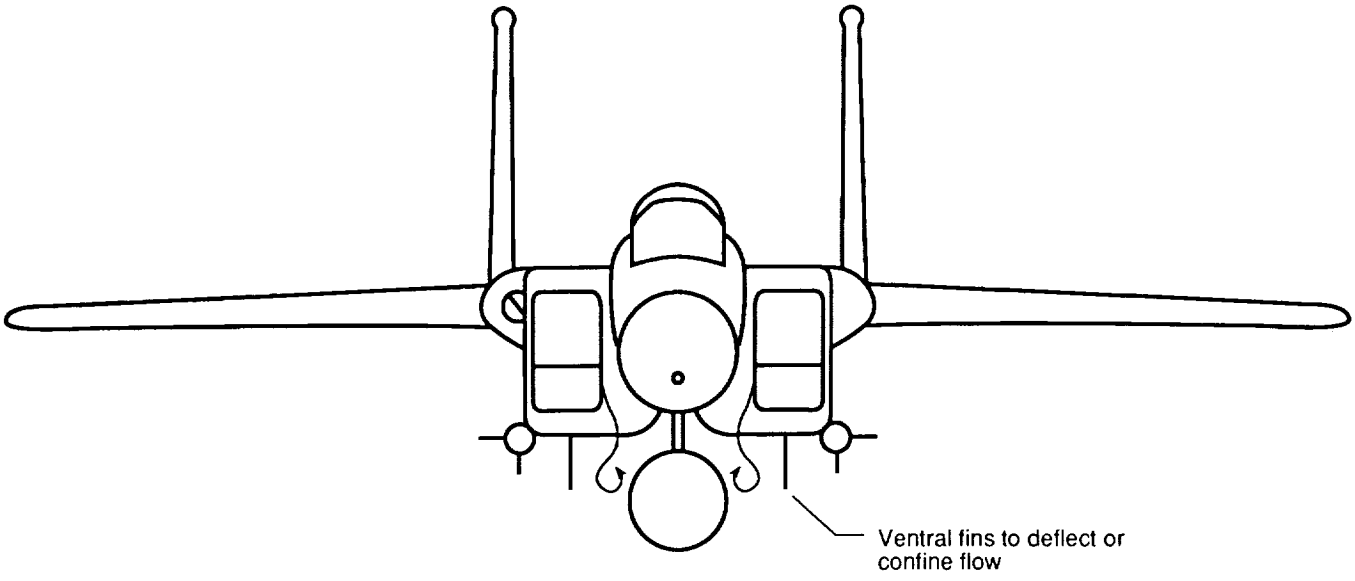

Figure 2. Vortex deflection method.

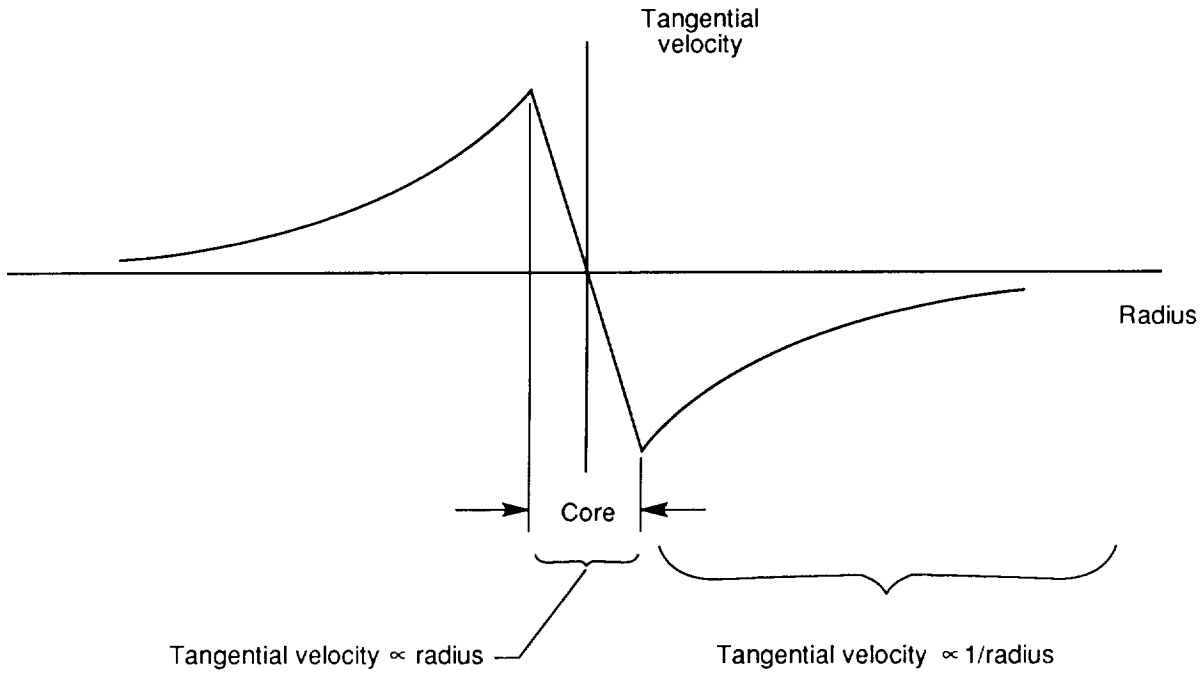

Figure 3. Ideal vortex tangential velocity profile.

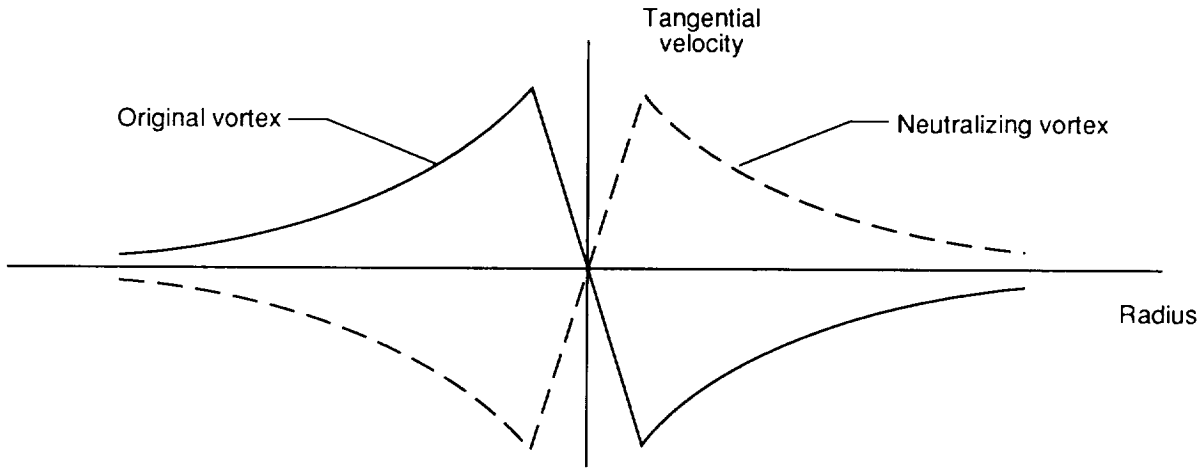

Figure 4. Neutralization ("unwinding") of vortex flow.

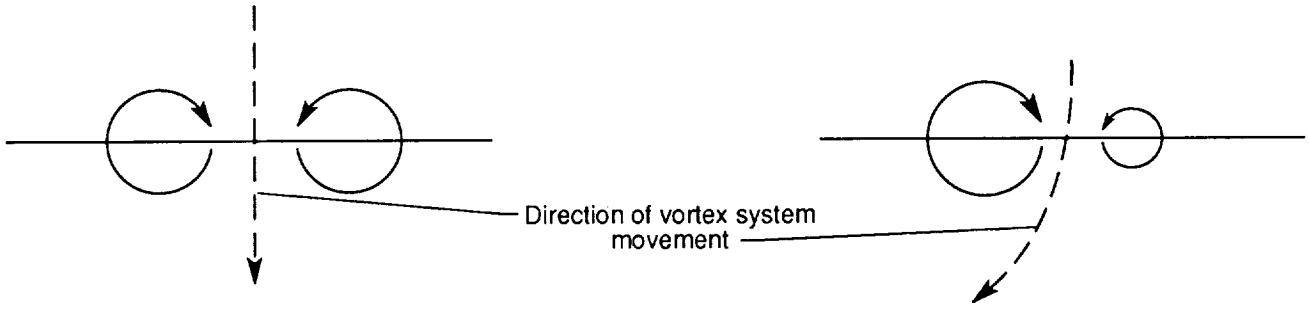

(a) Equal strength vortices. (b) Unequal strength vortices.

Figure 5. Mutual induction by vortices.

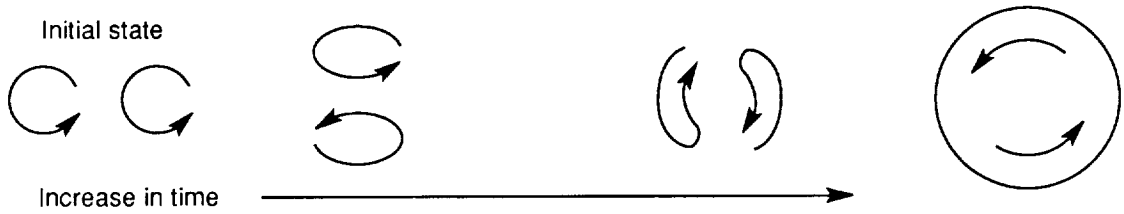

(a) Vortices of equal strength.

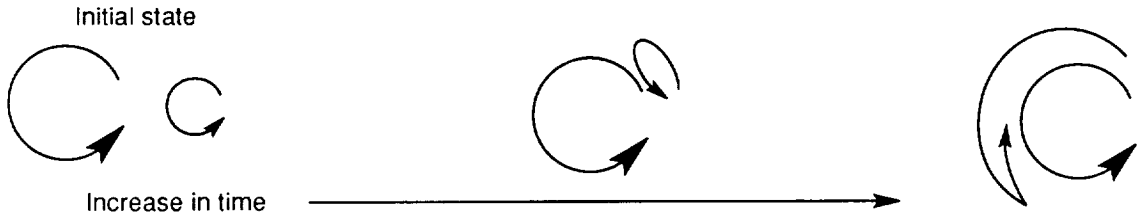

(b) Vortices of unequal strength.

Figure 6. Deformation and displacement of vortices.

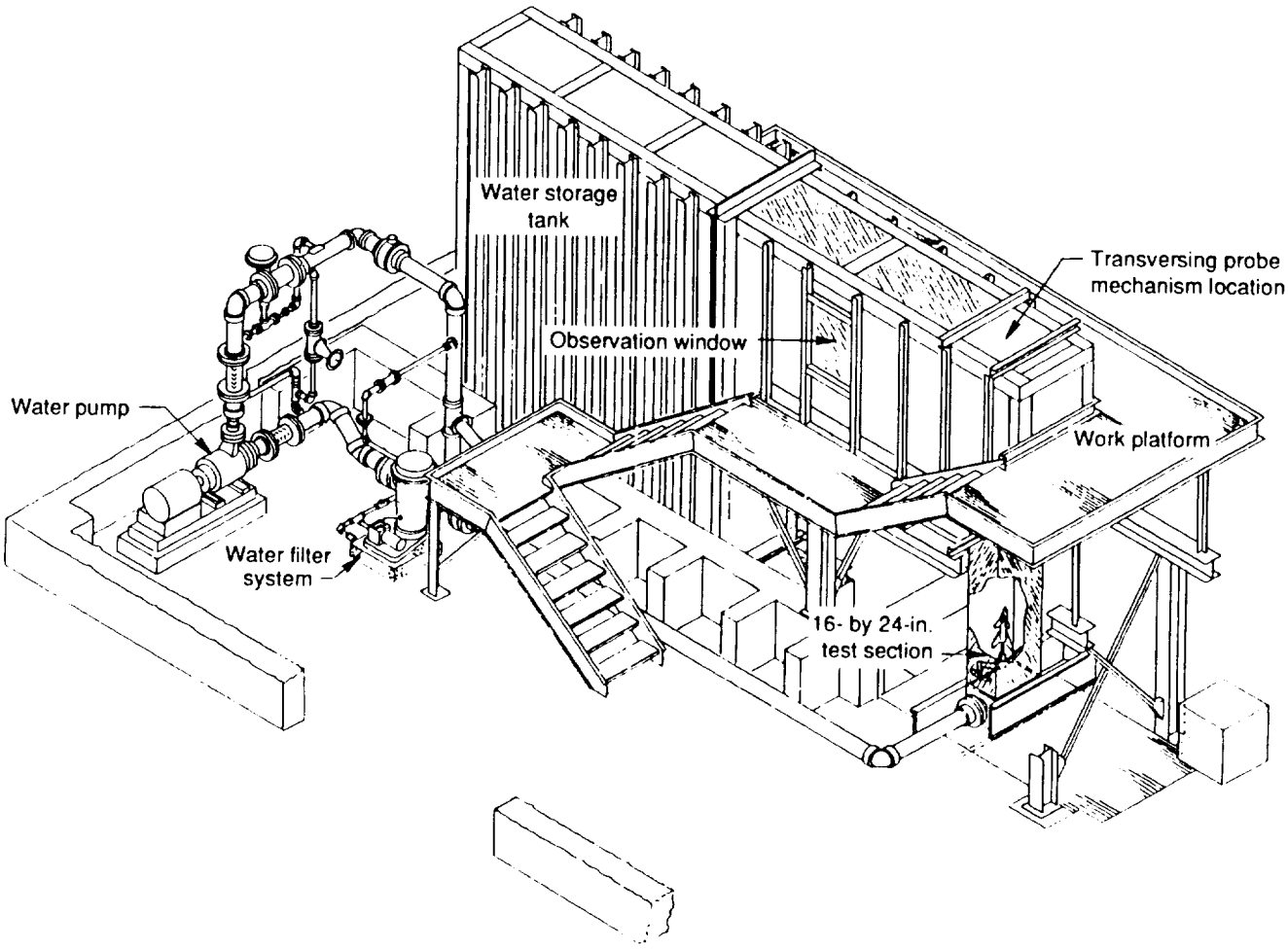

Figure 7. Langley 16- by 24-Inch Water Tunnel.

L-90-03

Figure 8. 1/48-scale model of twin-engine fighter.

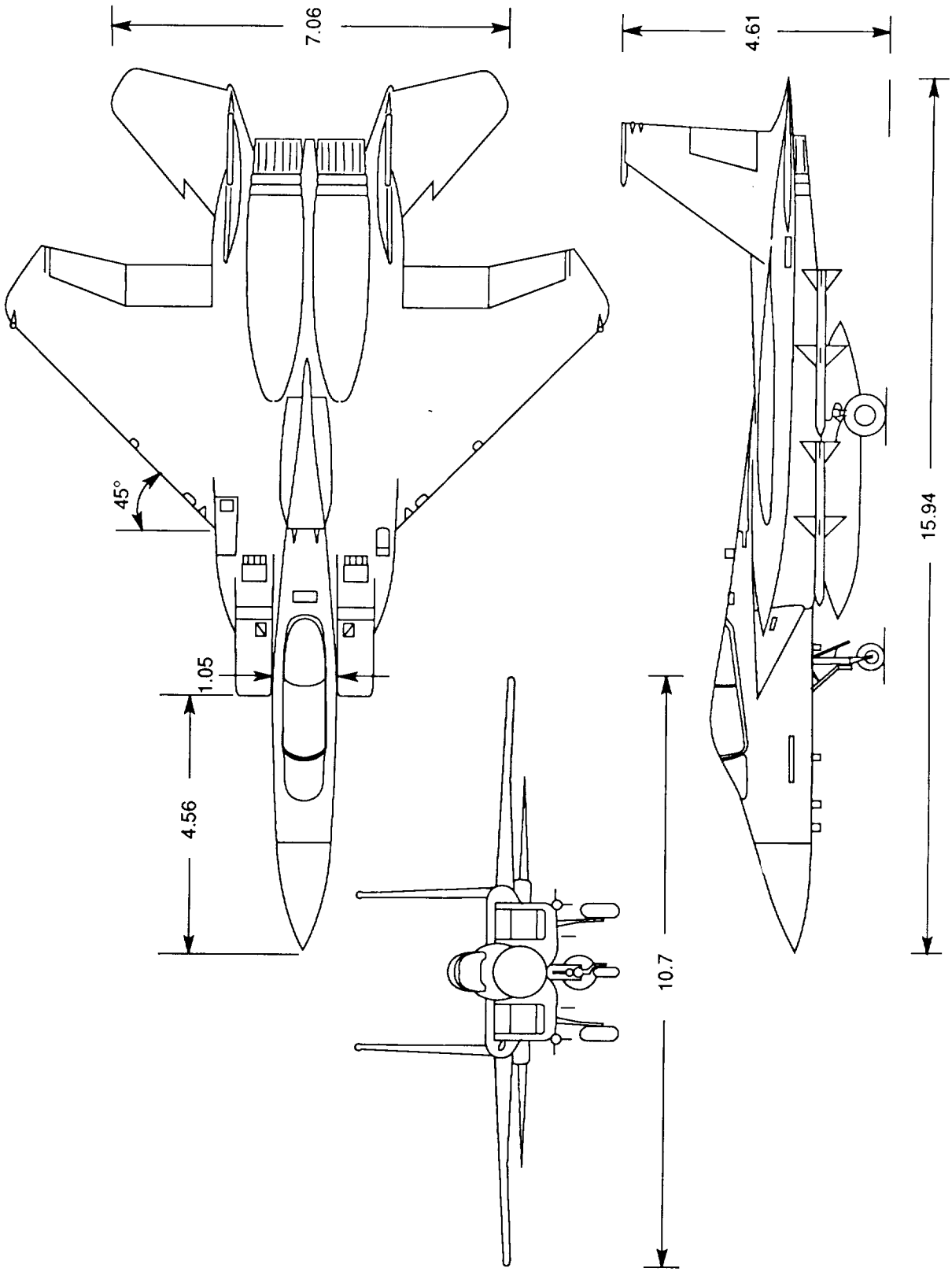

Figure 9. Three-view drawing of 1/48-scale twin-engine fighter. Dimensions in inches.

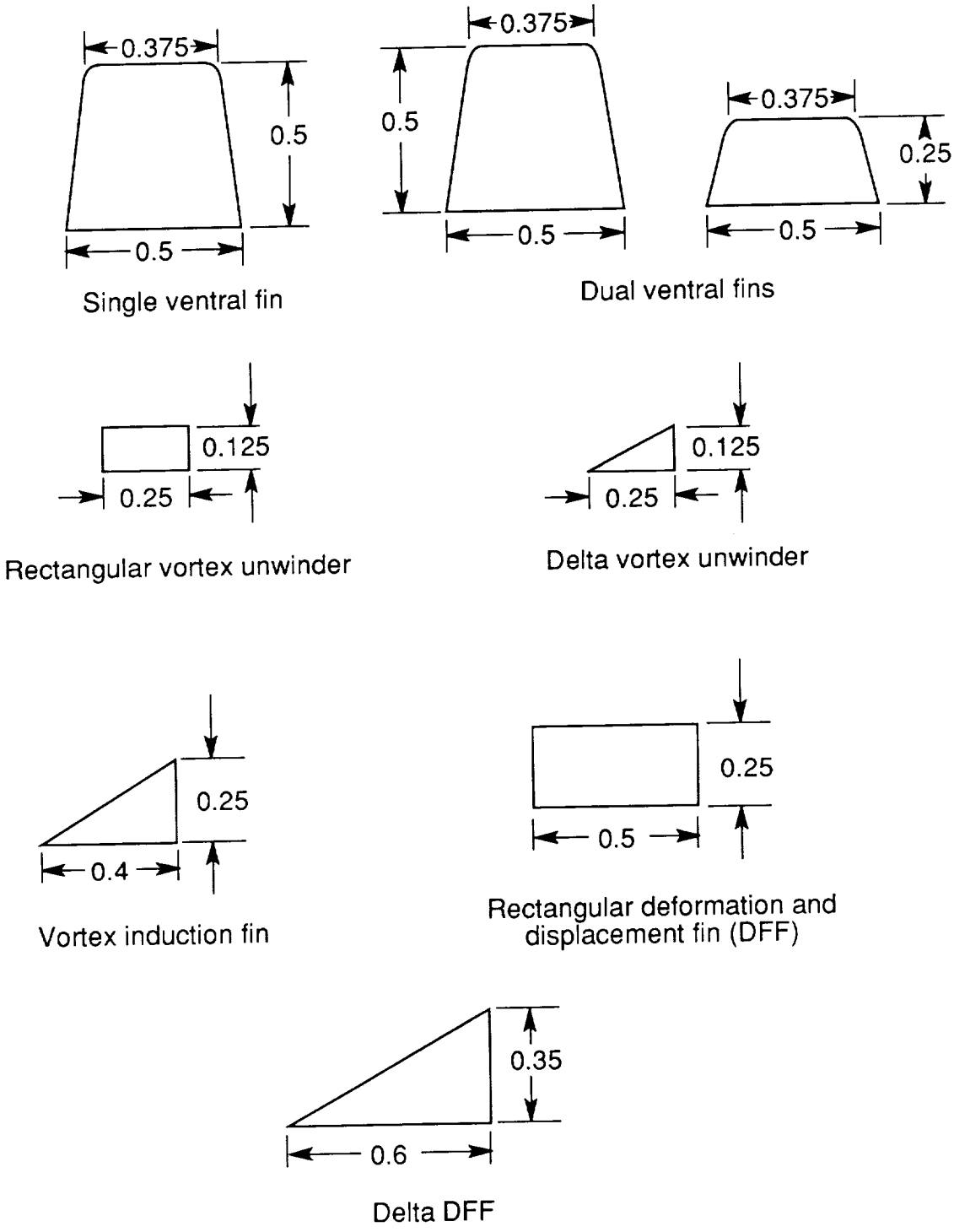

Figure 10. Flow control devices. Dimensions in inches.

ORIGINAL PAGE
BLACK AND WHITE PHOTOGRAPH

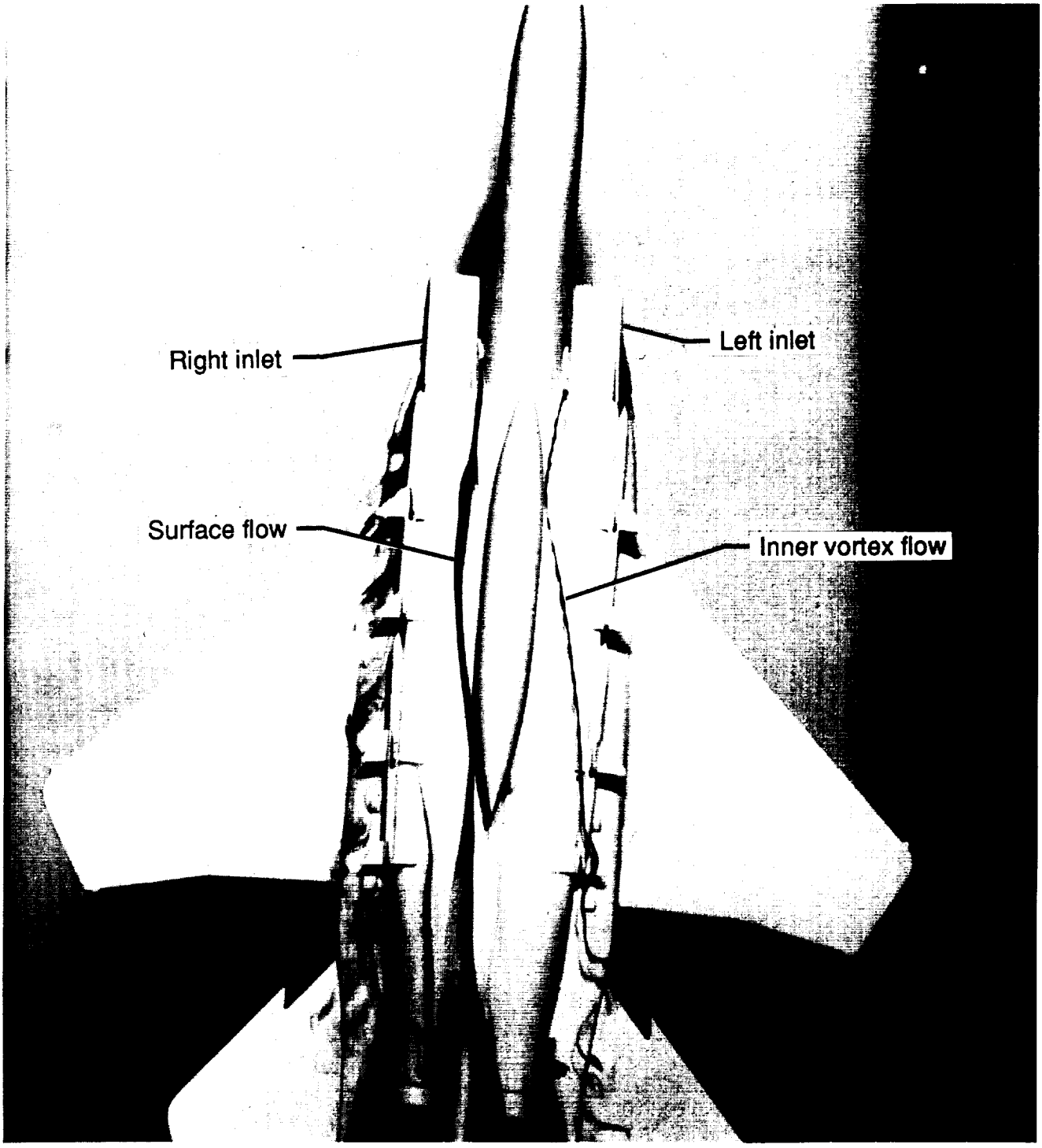

L-90-04

(a) Bottom view. $\alpha = 10°$.

Figure 11. Spillage flow around inlet. $\dot{m}_I/\dot{m}_\infty = 0.25$; $\beta = 5°$.

ORIGINAL PAGE
BLACK AND WHITE PHOTOGRAPH

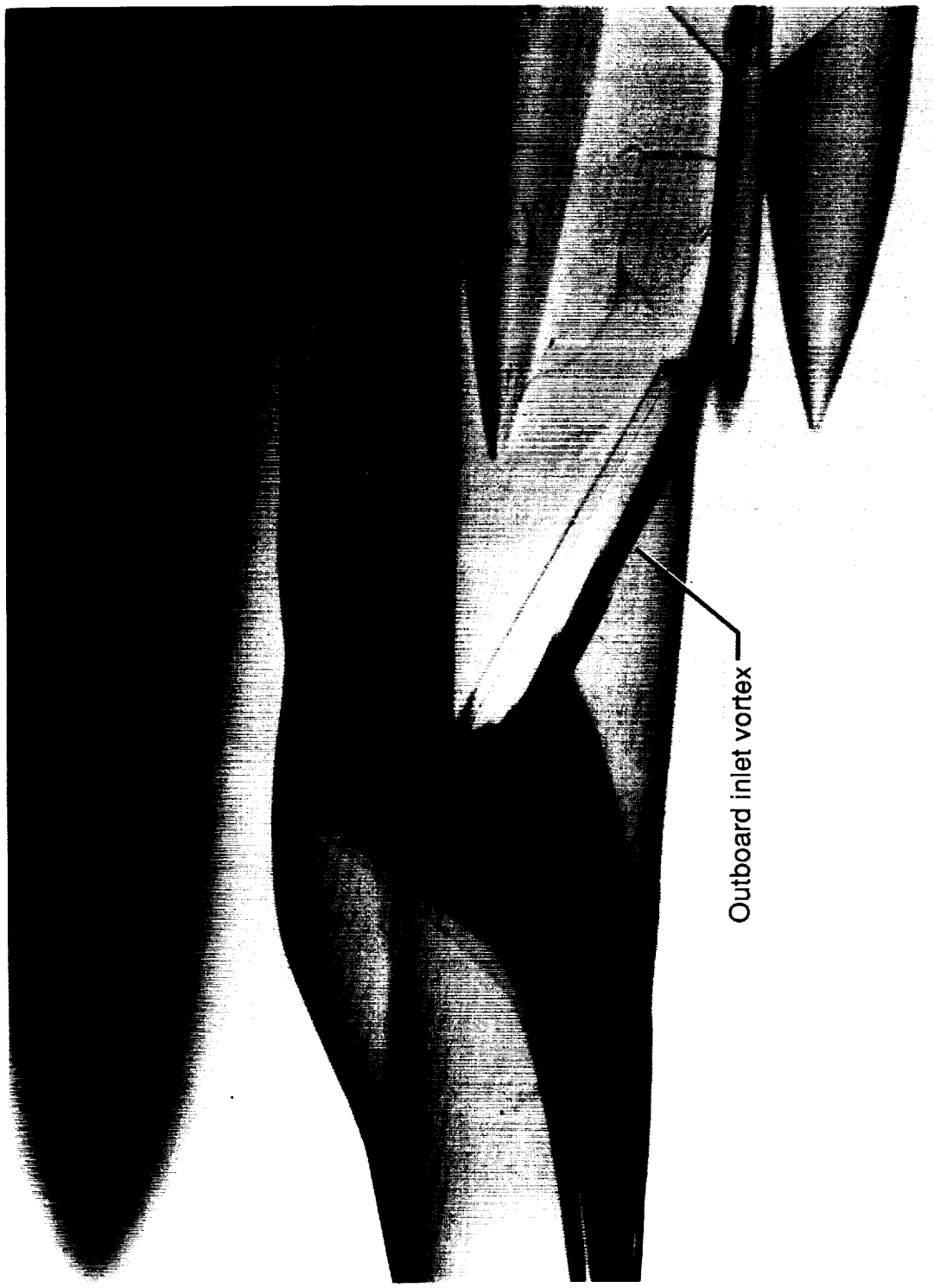

L-90-05

(b) Left side close-up. $\alpha = 5°$.

Figure 11. Continued.

ORIGINAL PAGE
BLACK AND WHITE PHOTOGRAPH

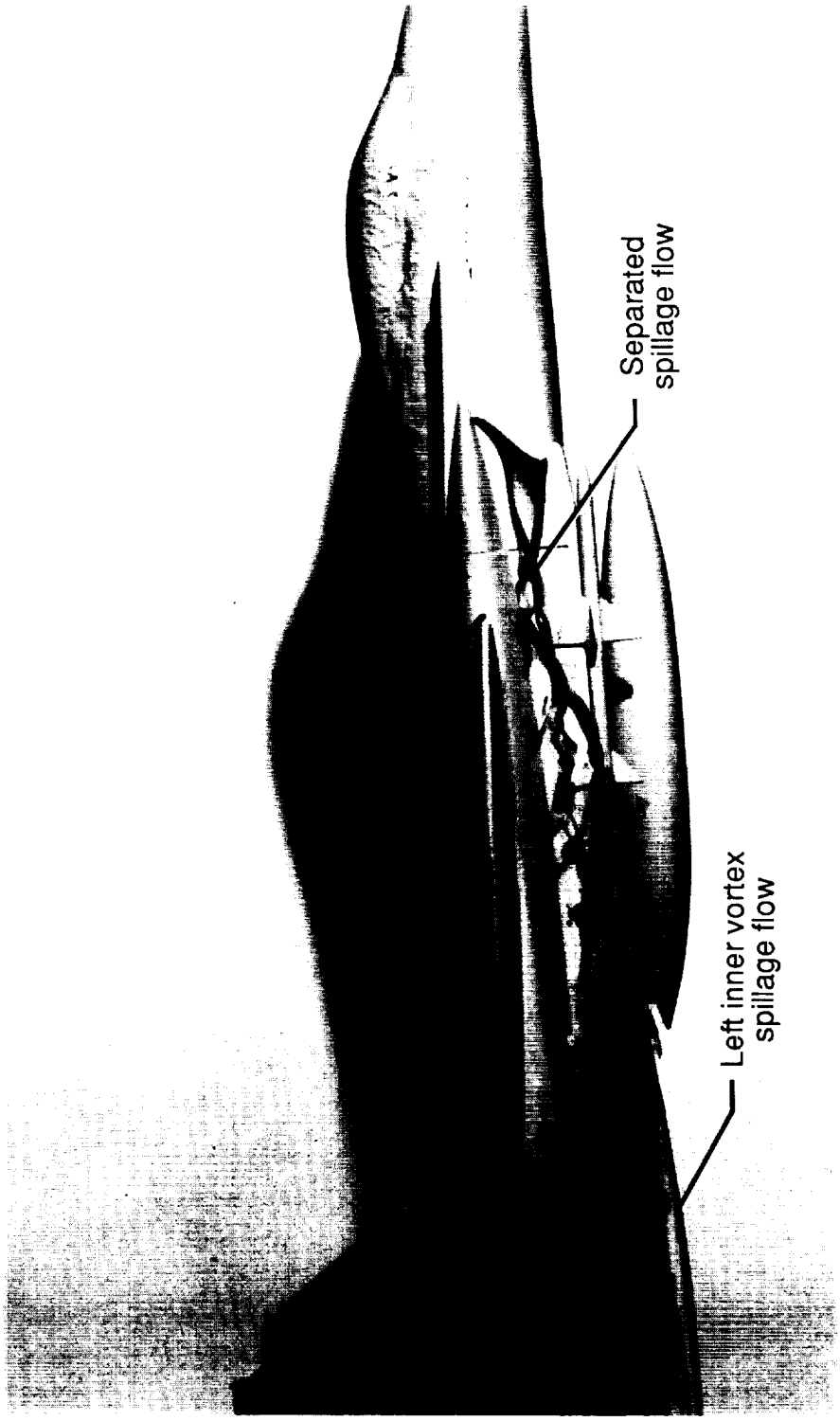

L-90-06

(c) Right side view. $\alpha = 5°$.

Figure 11. Concluded.

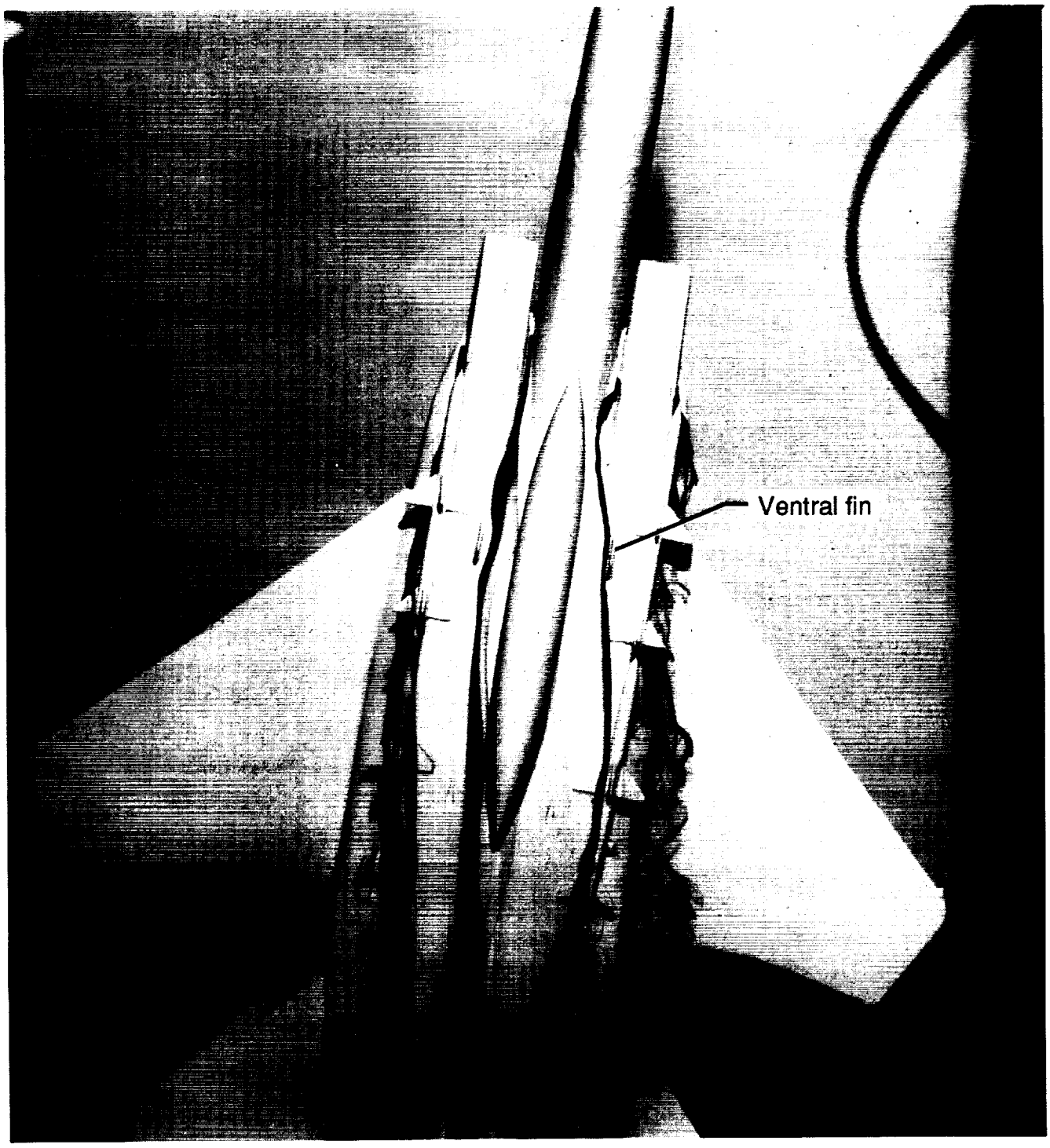

L-90-07

Figure 12. Forward single ventral fins. $\dot{m}_I/\dot{m}_\infty = 0.25$; $\alpha = 5°$; $\beta = 10°$.

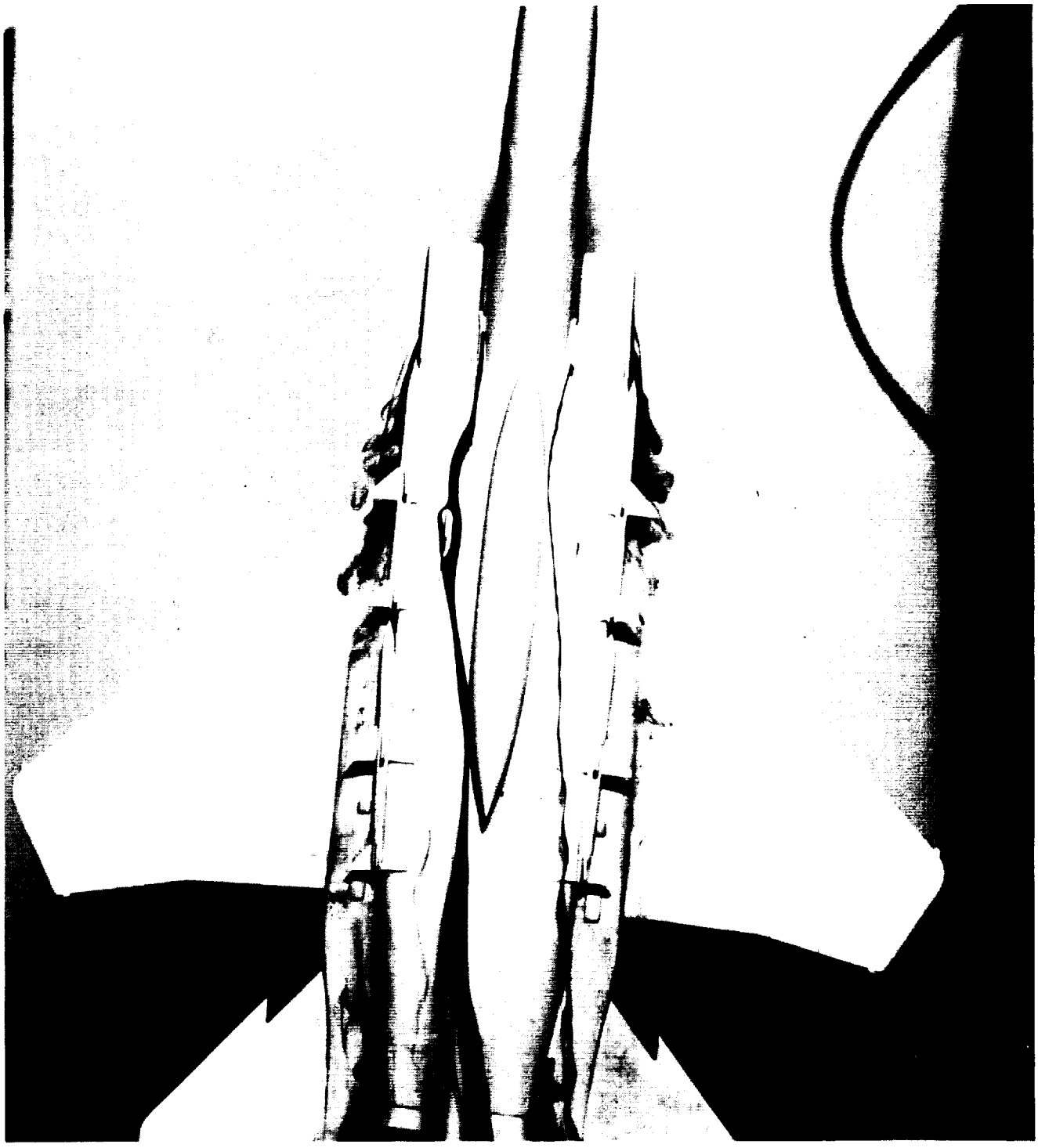

L-90-08

Figure 13. Forward single ventral fins. $\dot{m}_I/\dot{m}_\infty = 0.25$; $\alpha = 10°$; $\beta = 5°$.

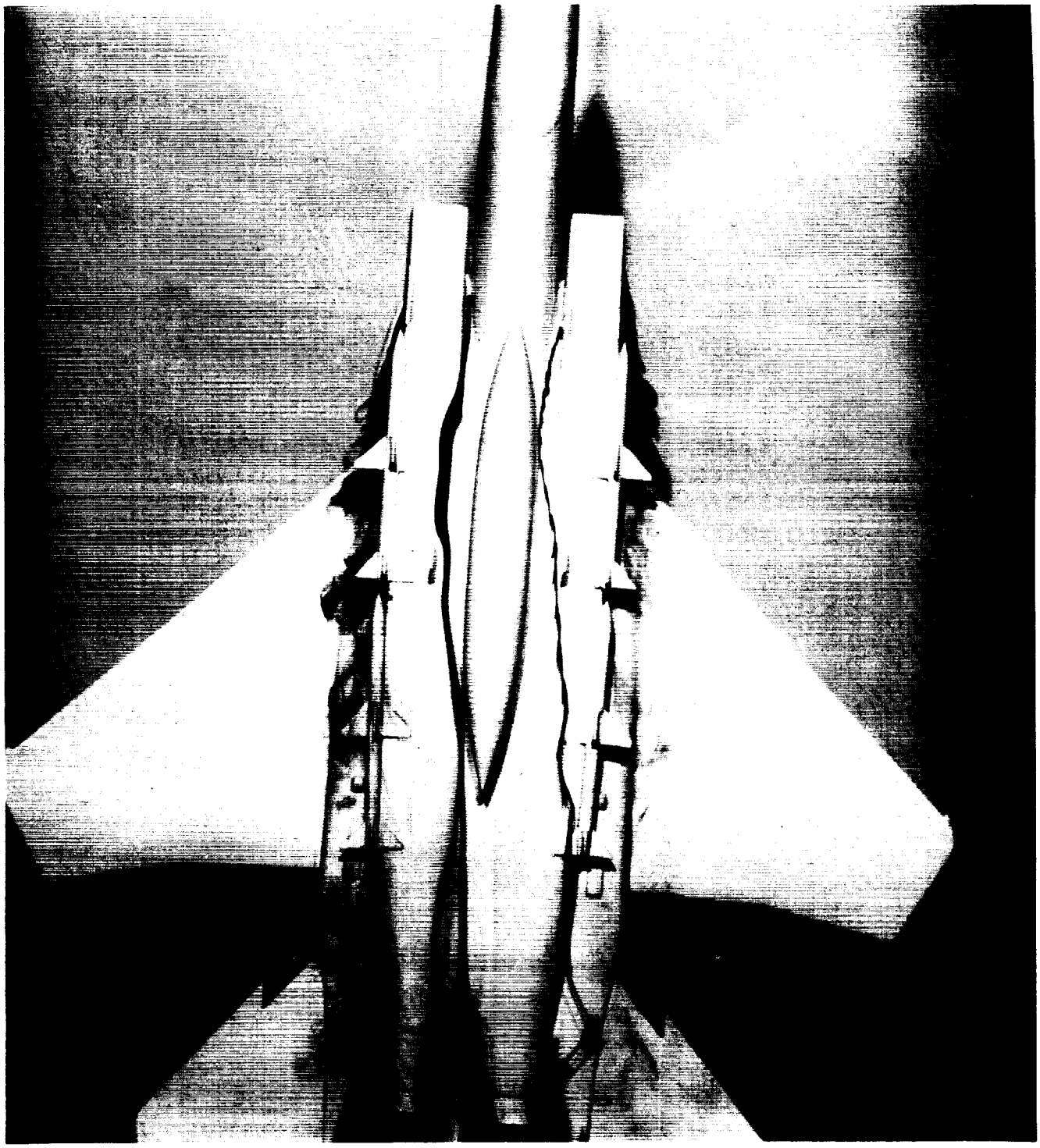

L-90-09

Figure 14. Aft single ventral fins. $\dot{m}_I/\dot{m}_\infty = 0.25$; $\alpha = 10°$; $\beta = 5°$.

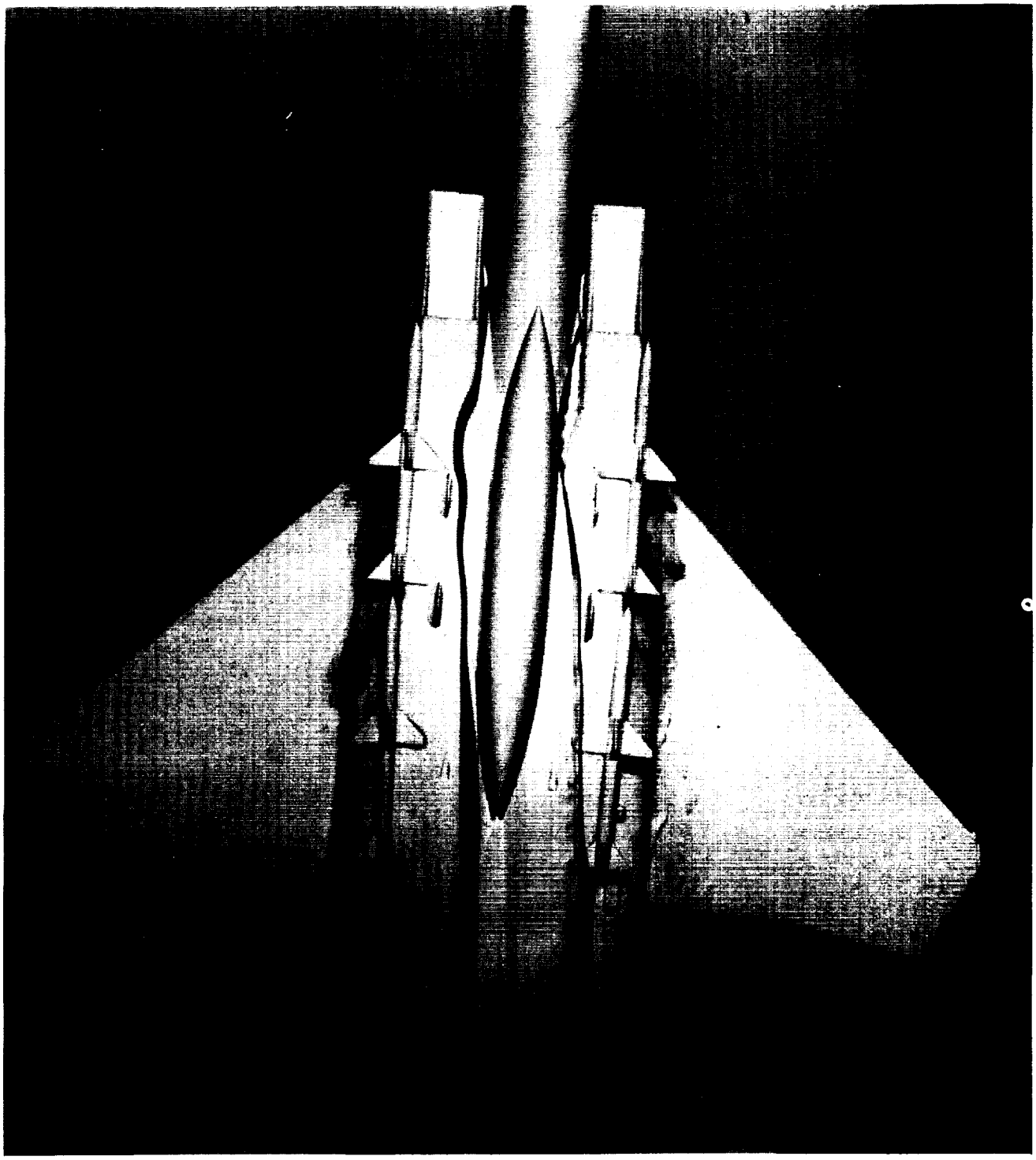

L-90-10

Figure 15. Double ventral fins. $\dot{m}_I/\dot{m}_\infty = 0.25$; $\alpha = 10°$; $\beta = 5°$.

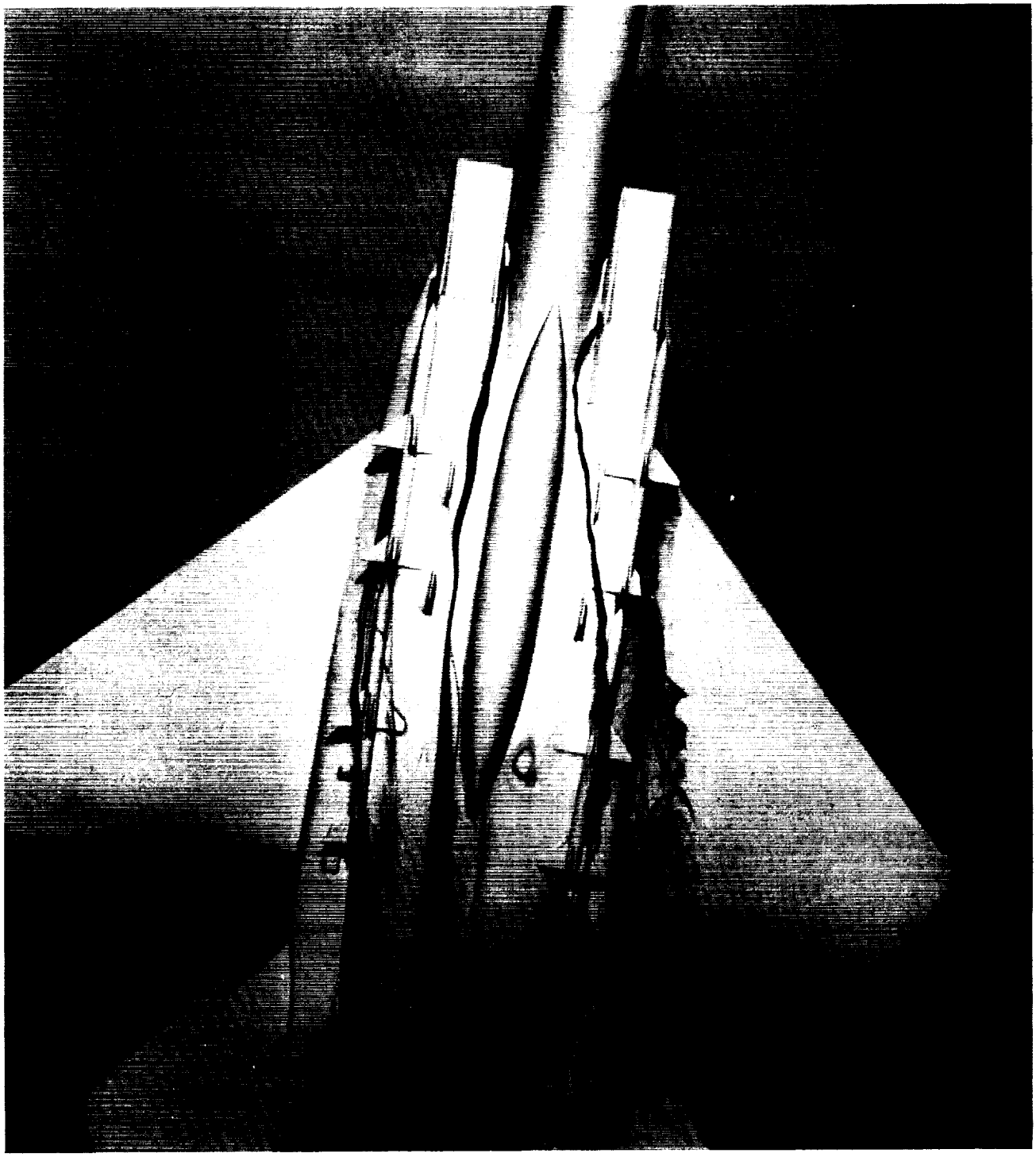

L-90-11

Figure 16. Double ventral fins. $\dot{m}_I/\dot{m}_\infty = 0.25$; $\alpha = 5°$; $\beta = 10°$.

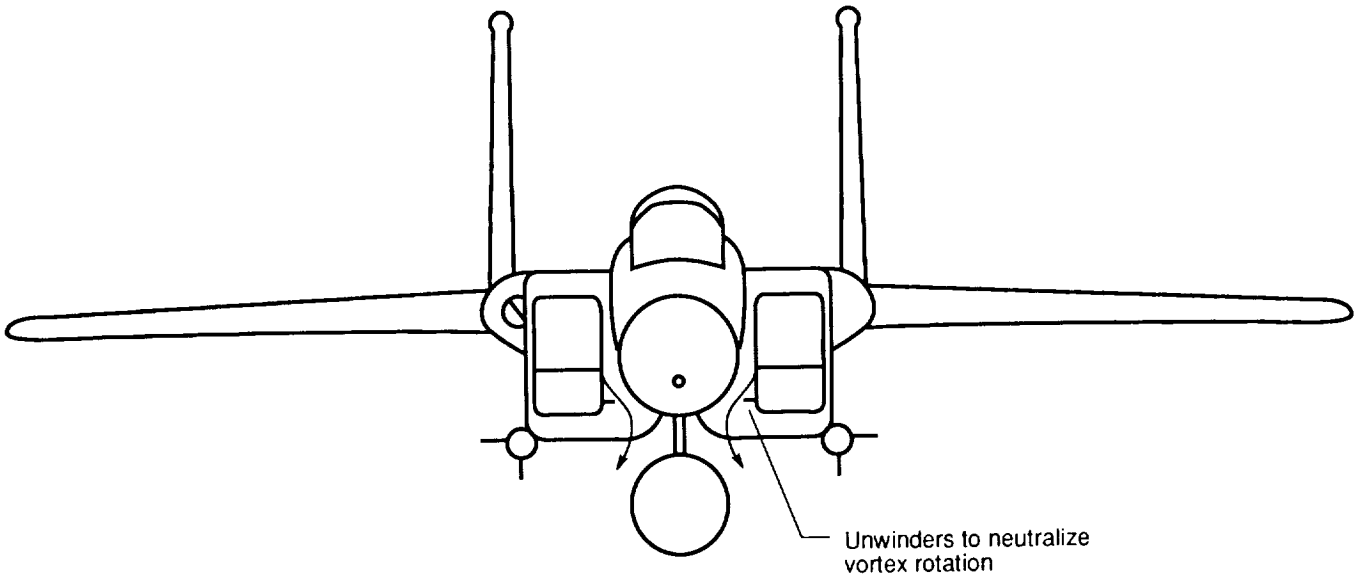

Figure 17. Vortex unwinders.

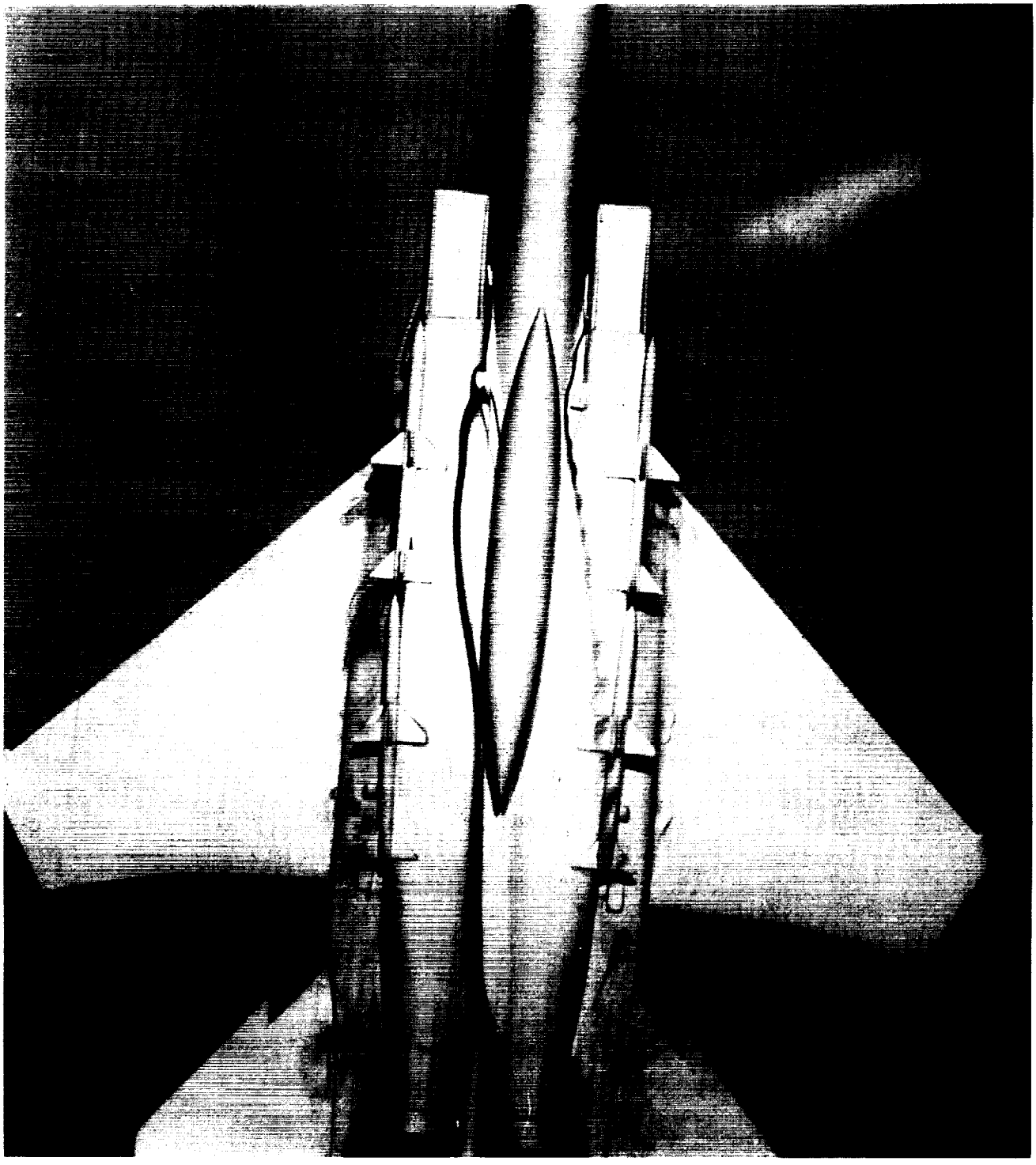

L-90-12

(a) Aft location.

Figure 18. Rectangular vortex unwinders. $\dot{m}_I/\dot{m}_\infty = 0.25$; $\alpha = 10°$; $\beta = 5°$.

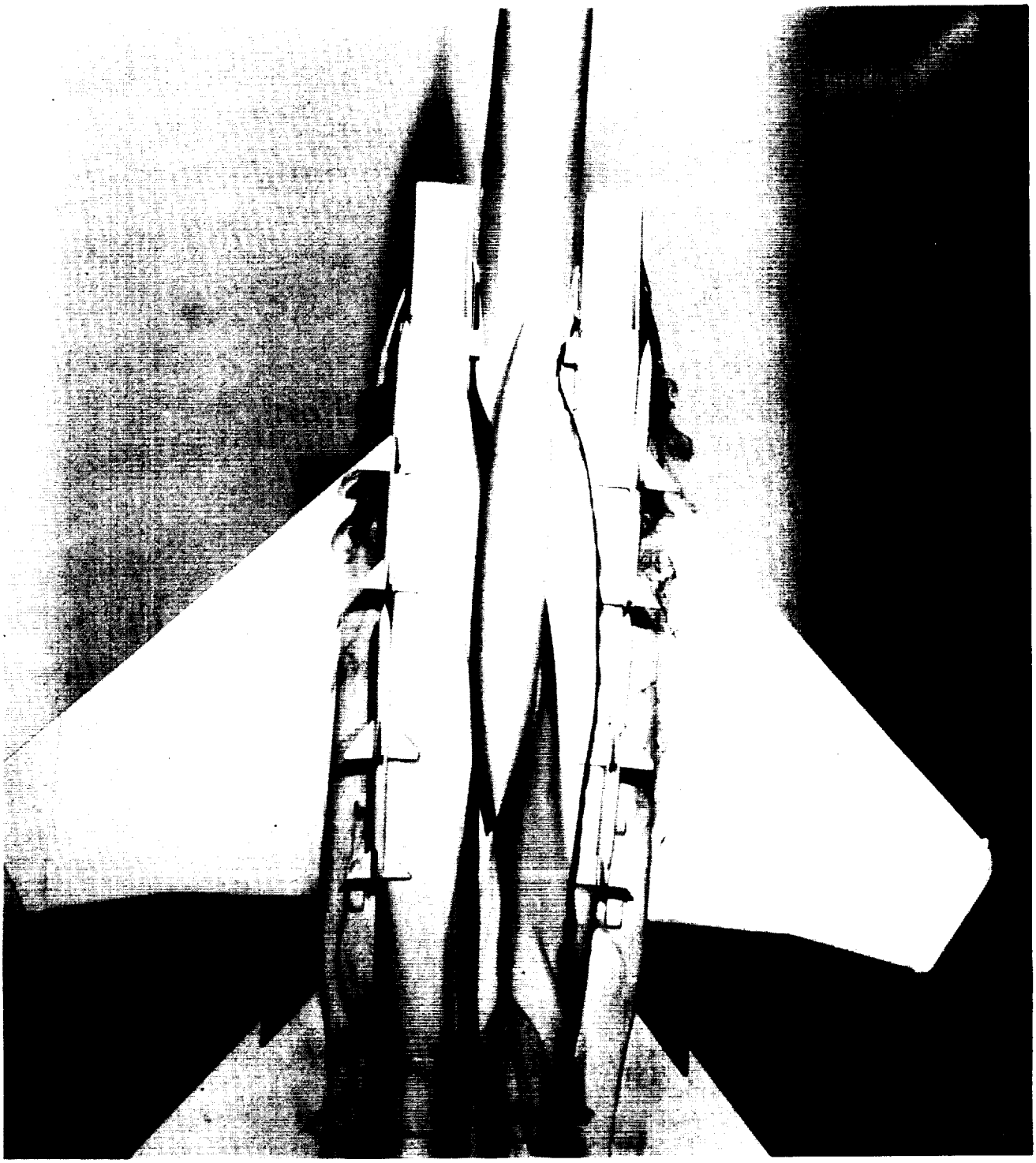

L-90-13

(b) Forward location.

Figure 18. Concluded.

ORIGINAL PAGE
BLACK AND WHITE PHOTOGRAPH

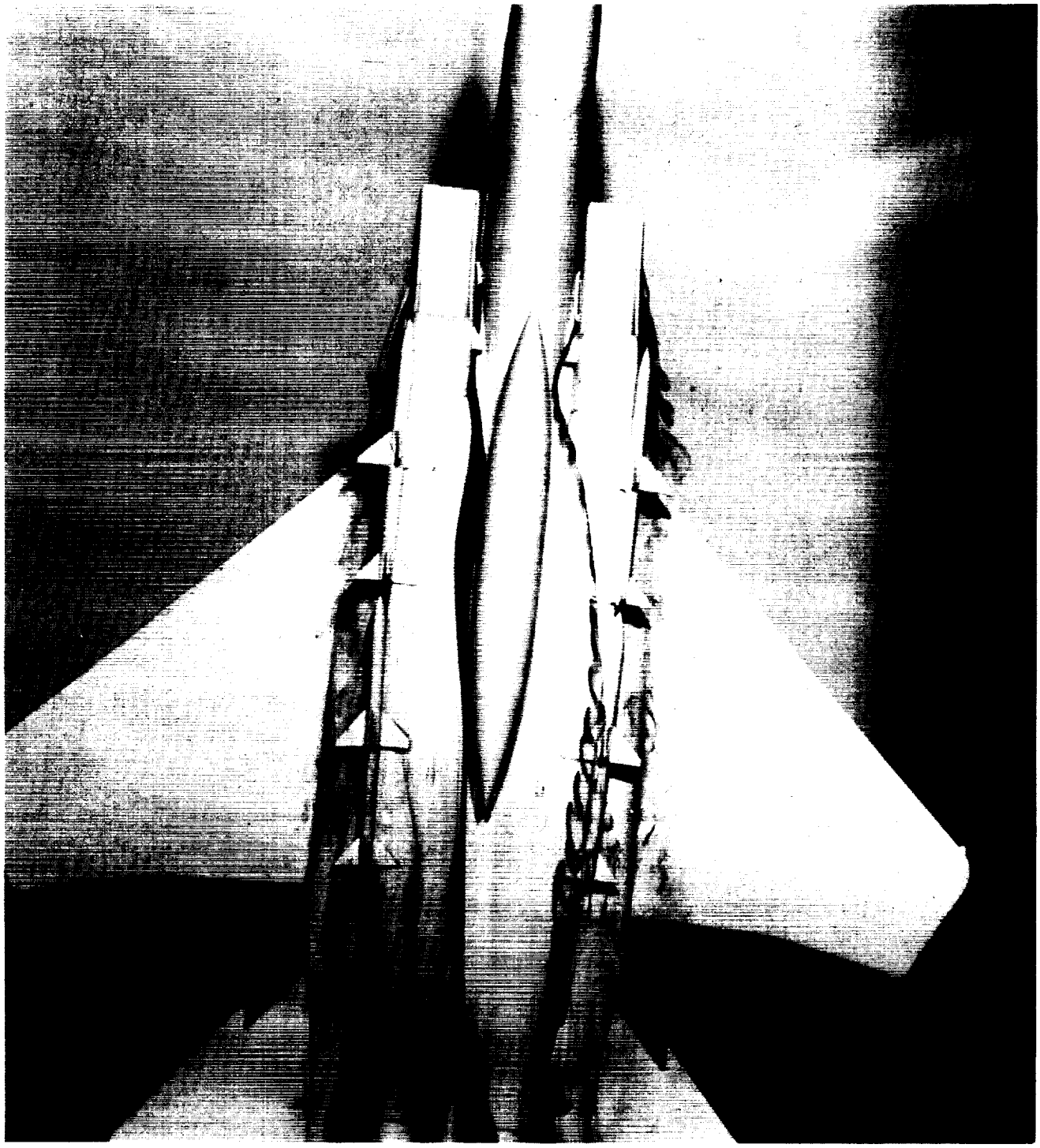

L-90-14

Figure 19. Semidelta vortex unwinders. $\dot{m}_I/\dot{m}_\infty = 0.25$; $\alpha = 10°$; $\beta = 5°$.

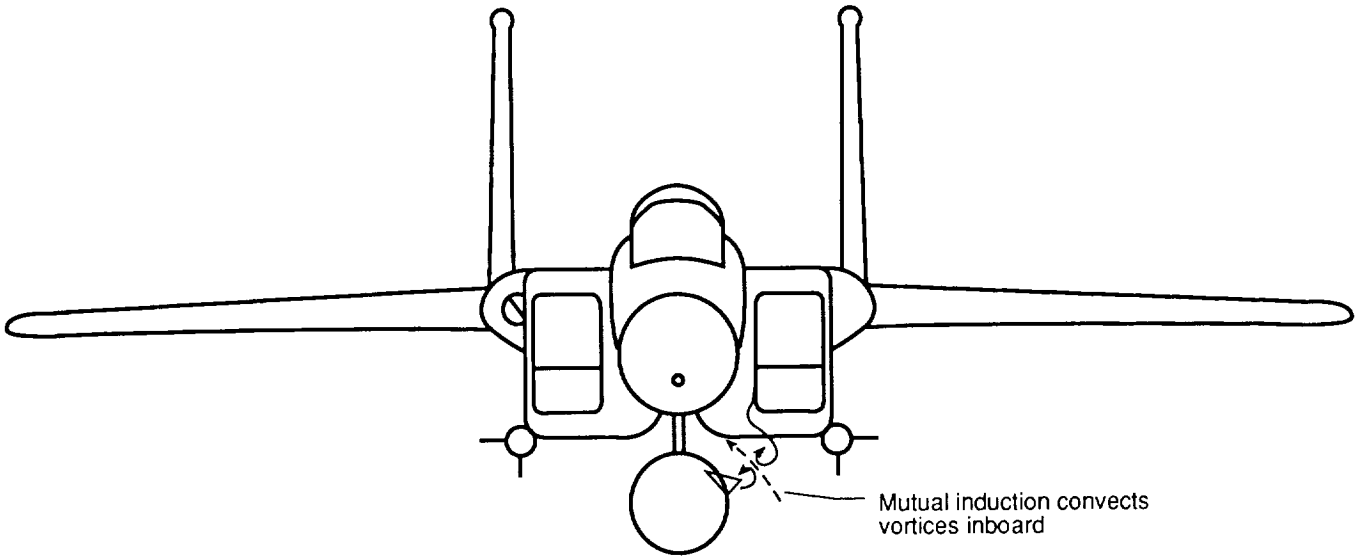

Figure 20. Vortex induction fins.

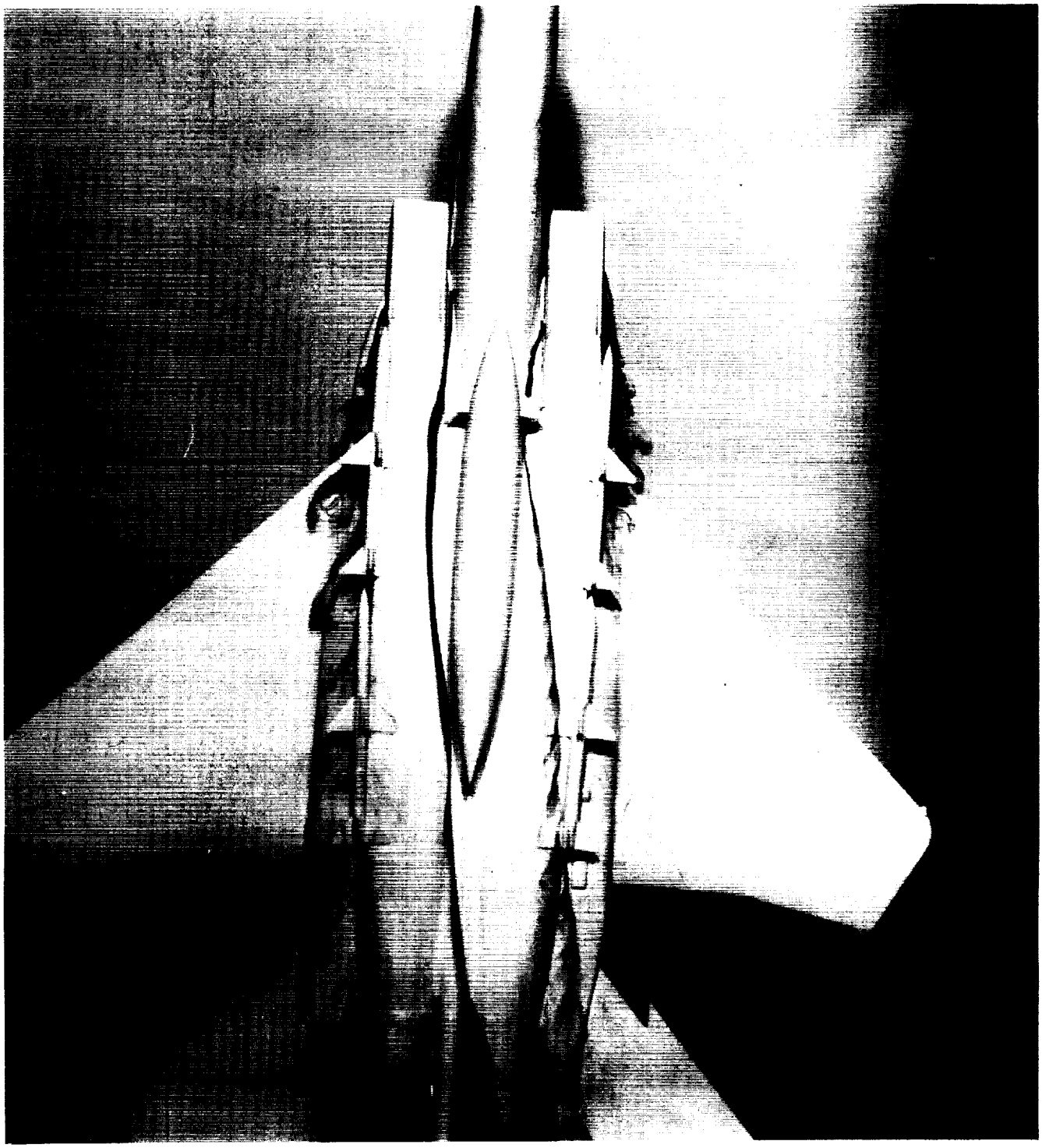

L-90-15

Figure 21. Vortex induction fuel tank fins. $\dot{m}_I/\dot{m}_\infty = 0.25$; $\alpha = 10°$; $\beta = 5°$.

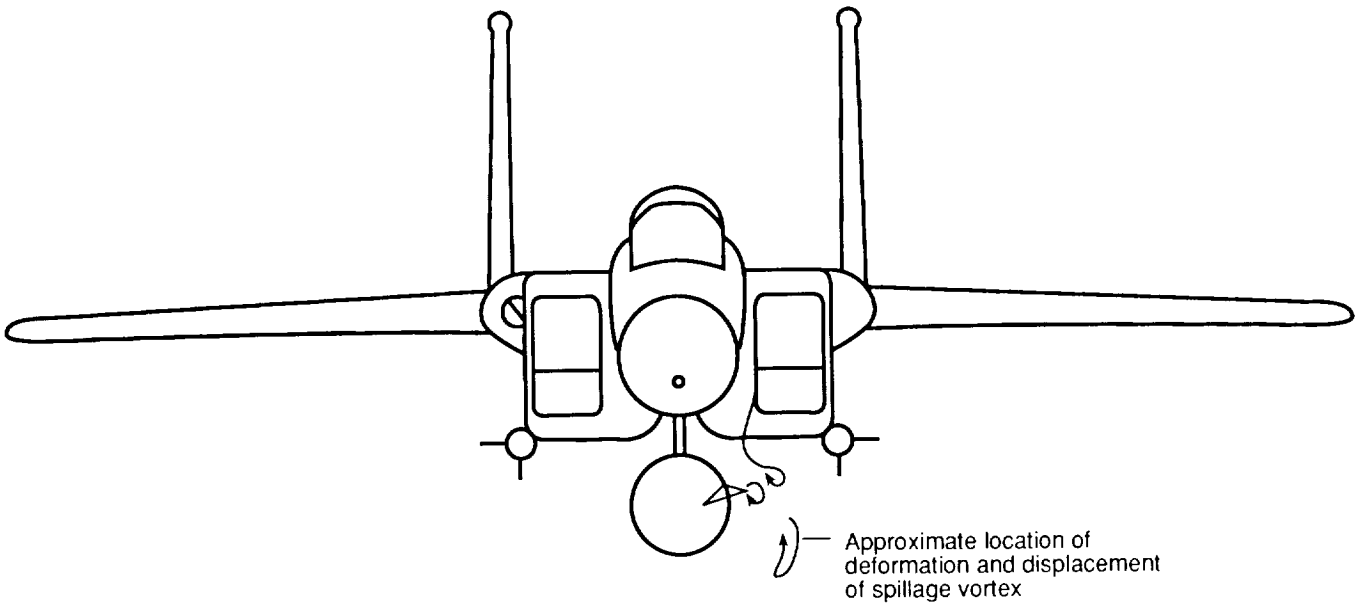

Figure 22. Deformation and displacement fins.

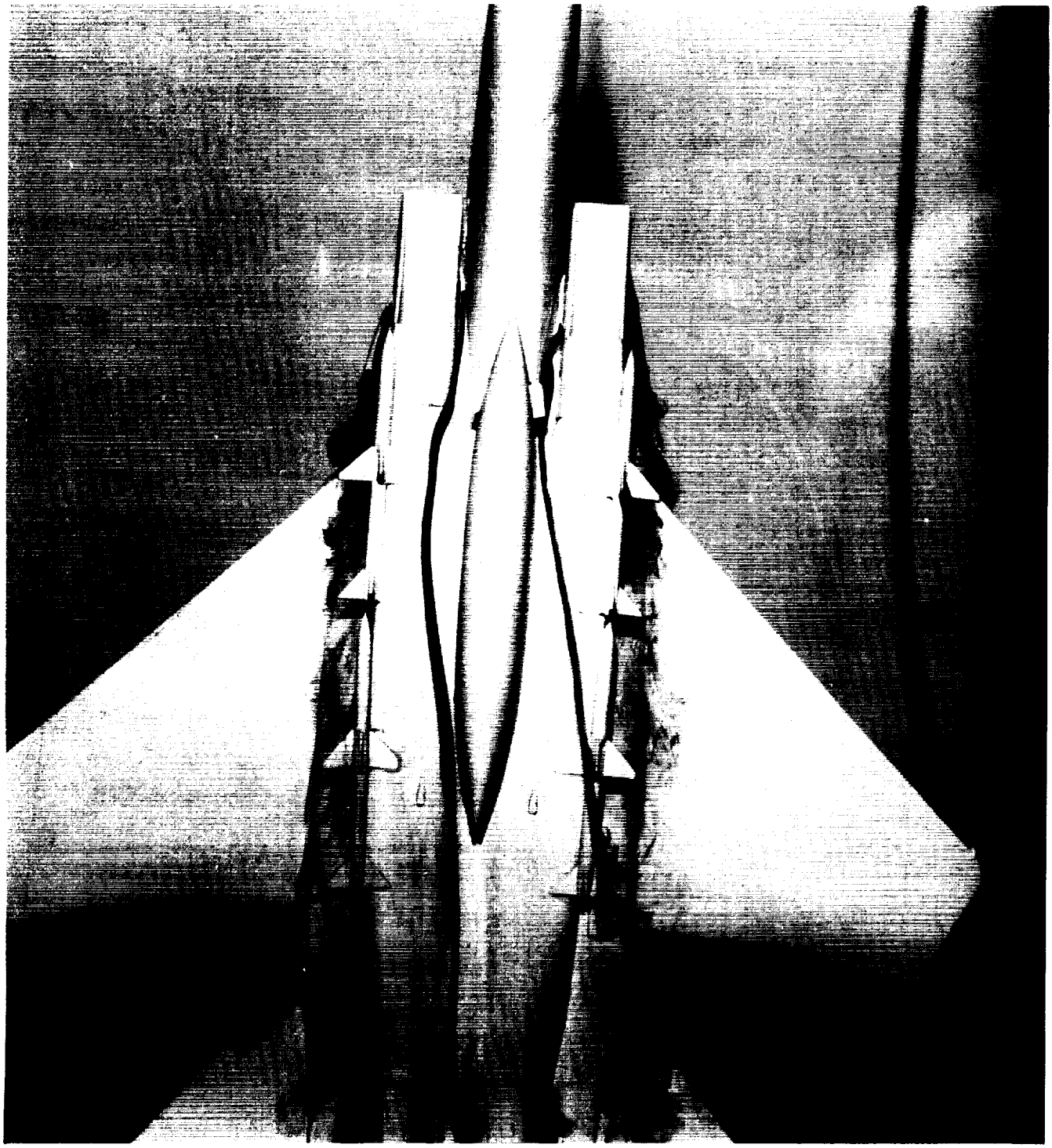

L-90-16

(a) Bottom view.

Figure 23. Deformation and displacement fins. $\dot{m}_I/\dot{m}_\infty = 0.25$; $\alpha = 10°$; $\beta = 5°$.

ORIGINAL PAGE
BLACK AND WHITE PHOTOGRAPH

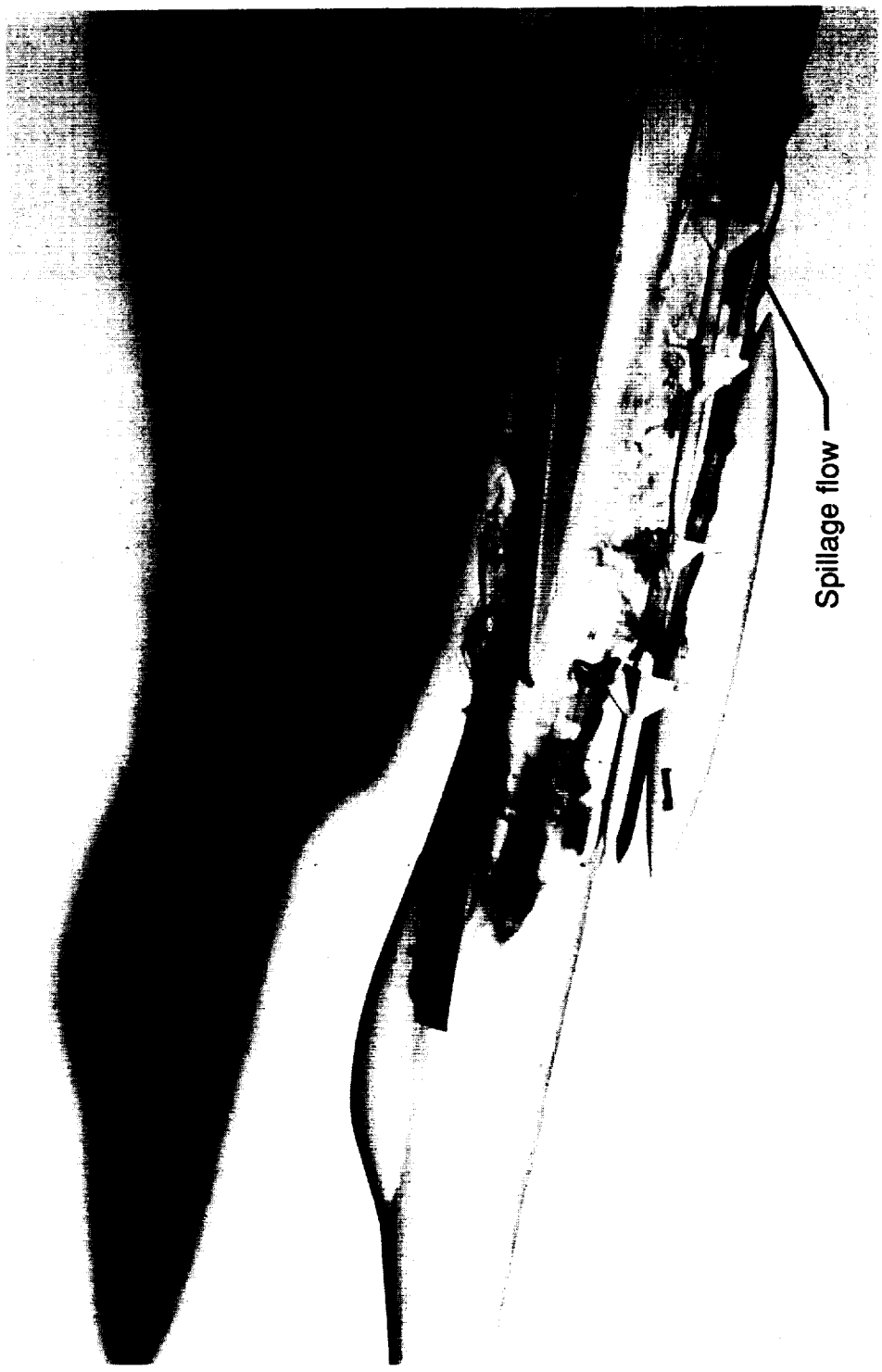

L-90-17

(b) Left side view.

Figure 23. Concluded.

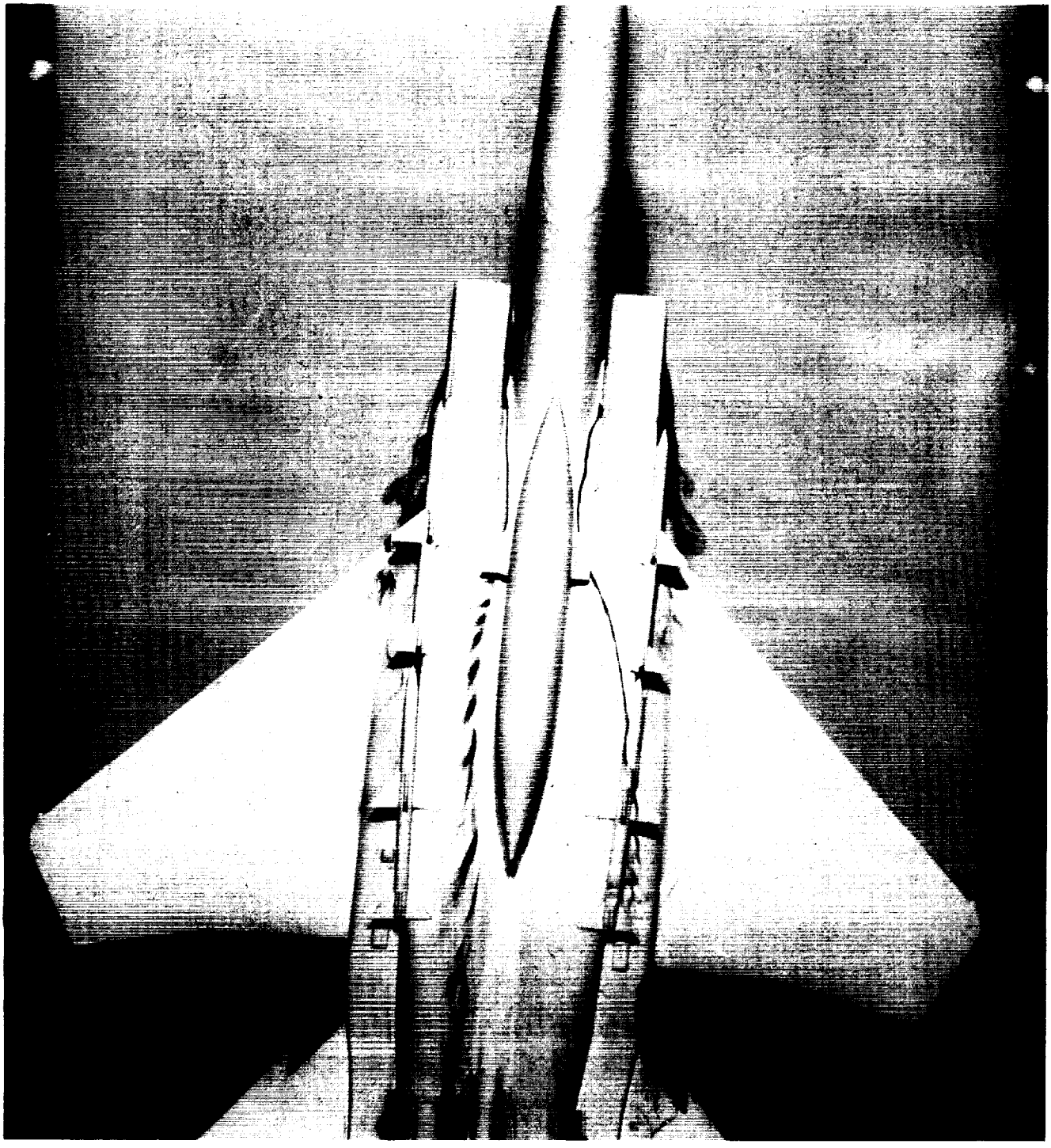

L-90-18

(a) Bottom view.

Figure 24. Aft deformation and displacement fins. $\dot{m}_I/\dot{m}_\infty = 0.25$; $\alpha = 10°$; $\beta = 5°$.

ORIGINAL PAGE
BLACK AND WHITE PHOTOGRAPH

L-90-19

(b) Left side view.

Figure 24. Concluded.

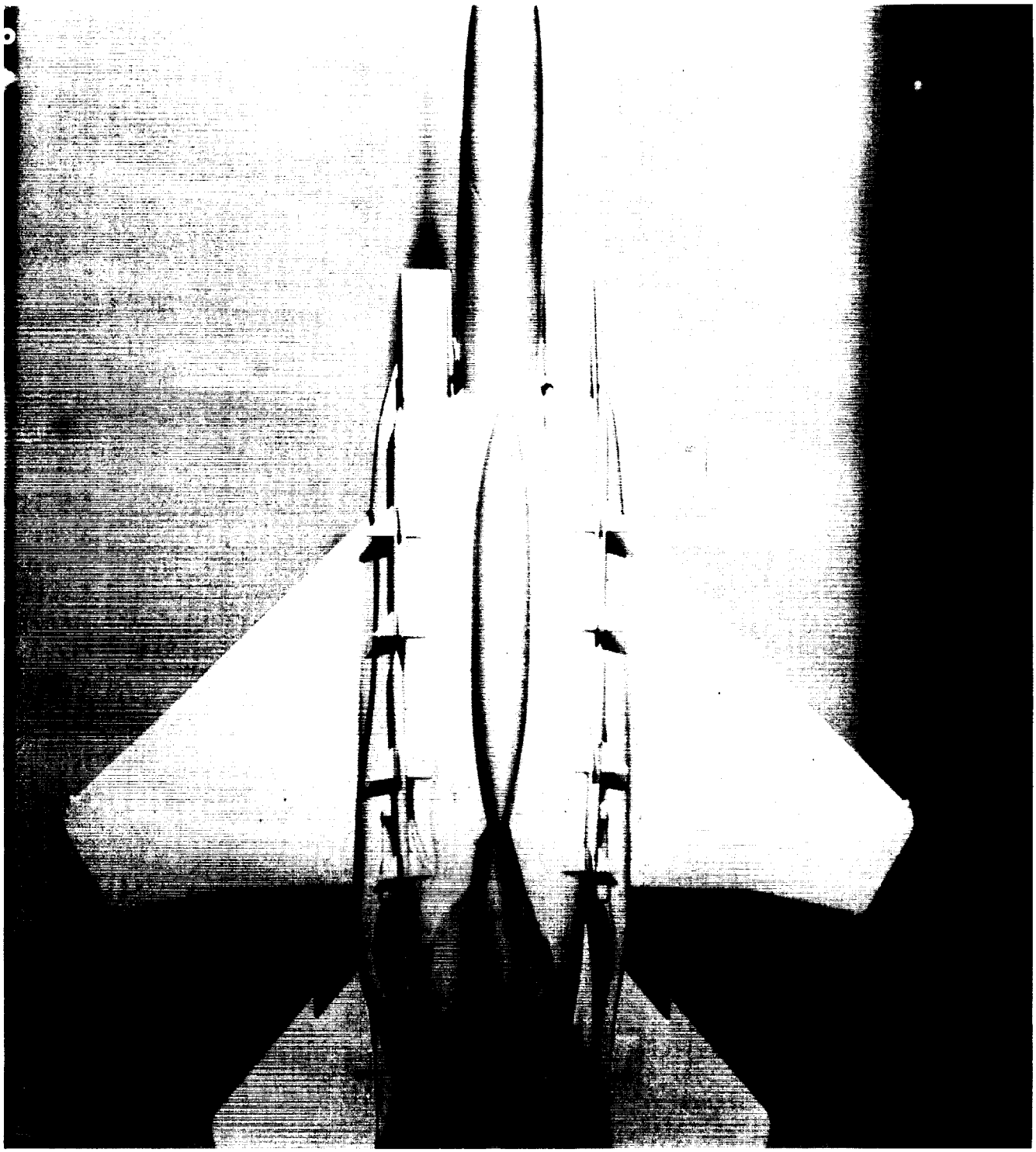

L-90-20

(a) $\beta = 0°$.

Figure 25. Fuel tank wake. $\alpha = 0°$.

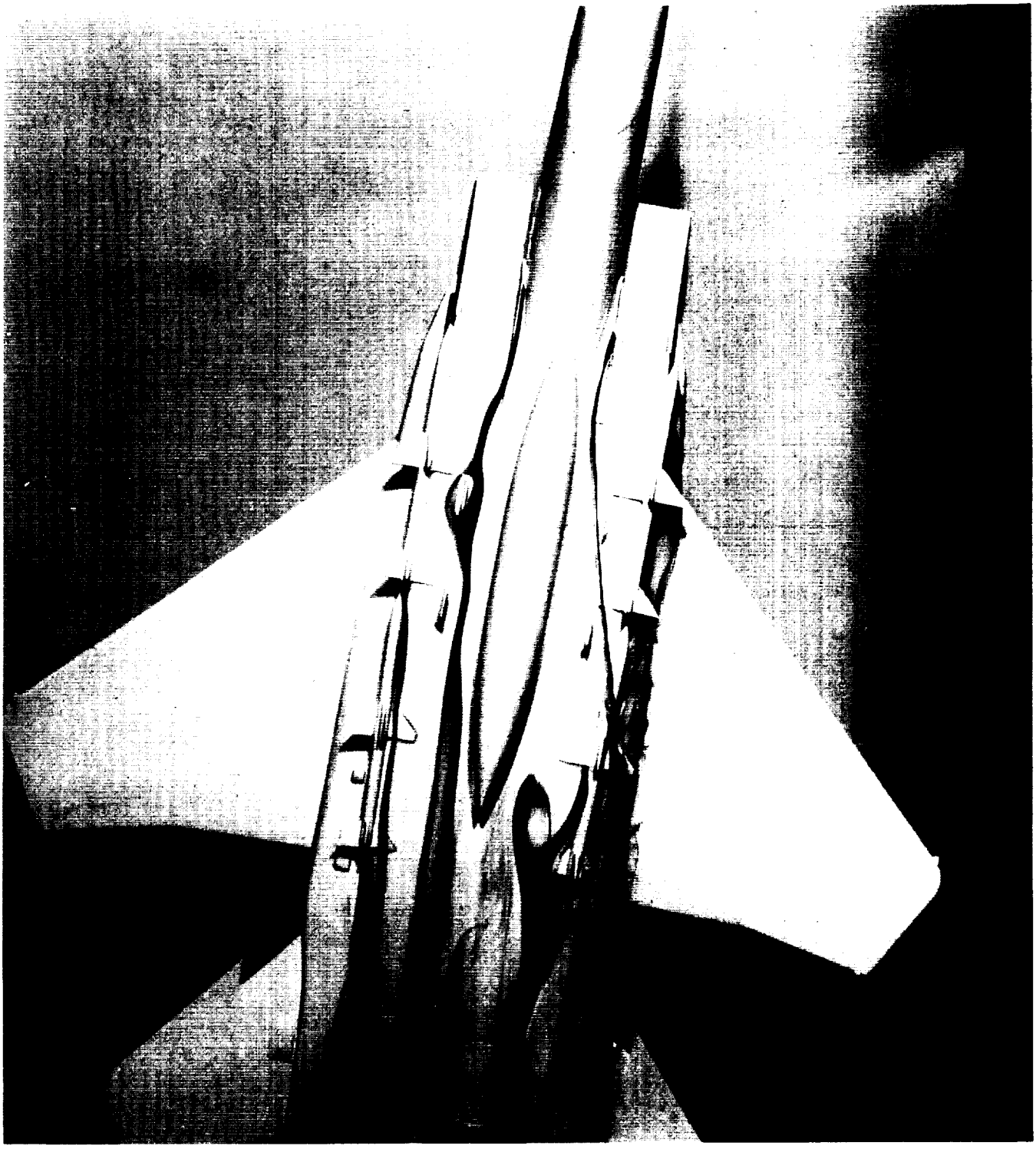

L-90-21

(b) $\beta = 10°$.

Figure 25. Concluded.

NASA
National Aeronautics and Space Administration

Report Documentation Page

1. Report No.	2. Government Accession No.	3. Recipient's Catalog No.
NASA TM-4181		

4. Title and Subtitle	5. Report Date
Water-Tunnel Investigation of Concepts for Alleviation of Adverse Inlet Spillage Interactions With External Stores	April 1990
	6. Performing Organization Code
7. Author(s)	8. Performing Organization Report No.
Dan H. Neuhart and Matthew N. Rhode	L-16710
9. Performing Organization Name and Address	10. Work Unit No.
NASA Langley Research Center Hampton, VA 23665-5225	505-62-71-01
	11. Contract or Grant No.
12. Sponsoring Agency Name and Address	13. Type of Report and Period Covered
National Aeronautics and Space Administration Washington, DC 20546-0001	Technical Memorandum
	14. Sponsoring Agency Code

15. Supplementary Notes

Dan H. Neuhart: Lockheed Engineering & Sciences Company, Hampton, Virginia.
Matthew N. Rhode: Langley Research Center, Hampton, Virginia.

16. Abstract

A test was conducted in the NASA Langley 16- by 24-Inch Water Tunnel to study alleviation of the adverse interactions of inlet spillage flow with the external stores of a fighter aircraft. A 1/48-scale model of a fighter aircraft was used to simulate the flow environment around the aircraft inlets and on the downstream underside of the fuselage. A controlled inlet mass flow was simulated by drawing water into the inlets. Various flow control devices were used on the underside of the aircraft model to manipulate the vortical inlet spillage flow.

17. Key Words (Suggested by Authors(s))	18. Distribution Statement
Water tunnel test Vortex flow Inlet spillage flow Flow visualization Flow manipulation	Unclassified Unlimited Subject Category 02

19. Security Classif. (of this report)	20. Security Classif. (of this page)	21. No. of Pages	22. Price
Unclassified	Unclassified	34	A03

For sale by the National Technical Information Service, Springfield, Virginia 22161-2171